



HAL
open science

Glomerular common gamma chain confers B- and T-cell-independent protection against glomerulonephritis

Yosu Luque, Dominique Cathelin, Sophie Vandermeersch, Xiaoli Xu, Julie Sohier, Sandrine Placier, Yi-Chun Xu-Dubois, Kevin Louis, Alexandre Hertig, Jean-Christophe Bories, et al.

► **To cite this version:**

Yosu Luque, Dominique Cathelin, Sophie Vandermeersch, Xiaoli Xu, Julie Sohier, et al.. Glomerular common gamma chain confers B- and T-cell-independent protection against glomerulonephritis. *Kidney International*, 2017, 91 (5), pp.1146 - 1158. 10.1016/j.kint.2016.10.037 . pasteur-01930924

HAL Id: pasteur-01930924

<https://pasteur.hal.science/pasteur-01930924>

Submitted on 22 Nov 2018

HAL is a multi-disciplinary open access archive for the deposit and dissemination of scientific research documents, whether they are published or not. The documents may come from teaching and research institutions in France or abroad, or from public or private research centers.

L'archive ouverte pluridisciplinaire **HAL**, est destinée au dépôt et à la diffusion de documents scientifiques de niveau recherche, publiés ou non, émanant des établissements d'enseignement et de recherche français ou étrangers, des laboratoires publics ou privés.



Distributed under a Creative Commons Attribution - NonCommercial - ShareAlike 4.0 International License

Glomerular common gamma chain confers B and T cell-independent protection against glomerulonephritis

Yosu Luque^{1,2,3*}, M.D., Dominique Cathelin^{1,2,8*}, Ph.D., Sophie Vandermeersch^{1,2}, B.S., Xiaoli Xu^{1,2}, M.D., Julie Sohier^{1,2}, M.D., Sandrine Placier^{1,2}, B.S., Yi-Chun Xu-Dubois¹, M.D., Kevin Louis³, B.S., Alexandre Hertig^{1,2,3}, M.D., Ph.D., Jean-Christophe Bories⁴, Ph.D., Florence Vasseur⁵, B.S., Fabien Campagne⁶, Ph.D., James P. Di Santo⁷, M.D., Ph.D., Christian Vosschenrich⁷, Ph.D., Eric Rondeau^{1,2,3} M.D., Ph.D. and Laurent Mesnard^{1,2,3,6} M.D., Ph.D.

¹ UMR_S 1155 Inserm, Rare and common kidney diseases, matrix remodeling and tissue repair, F-75020, Paris, France

² Sorbonne Universités, UPMC Univ Paris 06, France

³Assistance Publique - Hôpitaux de Paris, Urgences Néphrologiques et Transplantation Rénale, Hôpital Tenon, F-75020, Paris, France

⁴Inserm UMR 1126, Institut Universitaire d'Hématologie, Hôpital St. Louis, Paris, France

⁵Inserm U1020, Université Paris Descartes, 75014 Paris, France

⁶Weill Medical College of Cornell University, Institute of Computational Biomedicine, New York, NY 10065, USA

⁷Institut Pasteur, Unité Immunité innée and Inserm U668, 75724 Paris, France

⁸Imaging and Cytometry Facility of Tenon, UMR_S 1155 Inserm, Rare and common kidney diseases, matrix remodelling and tissue repair, F-75020, Paris, Sorbonne Universités, UPMC Univ Paris 06, France

* YL and DC contributed equally to this work.

Running title: Epithelial common gamma chain attenuates crescentic glomerulonephritis

Abstract word count: 240

Main body word count: 4775

Correspondence to:

Dr Laurent Mesnard, laurent.mesnard@aphp.fr ; Inserm UMR S1155, Hôpital Tenon, 4 rue de la Chine, 75020 Paris, France. Phone: 331 56 01 83 17; Fax 331 56 01 66 59

Abstract

Crescentic glomerulonephritis (GN) is a life threatening renal disease that has been extensively studied by the experimental anti-glomerular basement membrane glomerulonephritis (anti-GBM-GN) model. Although T cells have a significant role in this model, athymic/nude mice and rats still develop severe renal disease. Our aim was to explore further the contribution of intrinsic renal cells in the development of T cell-independent GN lesions. We induced anti-GBM-GN in 3 strains of immunodeficient mice (*Rag2*^{-/-}, *Rag2*^{-/-}*Il2rg*^{-/-} and *Rag2*^{-/-}*Il2rb*^{-/-}) which are devoid of either T/B cells or T/B/NK cells. *Rag2*^{-/-}*Il2rg*^{-/-} or *Rag2*^{-/-}*Il2rb*^{-/-} mice harbor an additional deletion of either the common gamma chain (γ C) or the interleukin-2 receptor β subunit (IL-2R β) respectively, impairing IL-15 signaling in particular. As expected, all these strains developed severe anti-GBM-GN. In addition, bone marrow replenishment experiments allowed us to deduce a protective role for the glomerular-expressed γ C during anti-GBM-GN. Given that IL-15 has been found highly expressed in nephritic kidneys despite the absence of lymphocytes, we then studied this cytokine *in vitro* on primary cultured podocytes from immunodeficient mice (*Rag2*^{-/-}*Il2rg*^{-/-} and *Rag2*^{-/-}*Il2rb*^{-/-}) compared to controls. IL-15 induces downstream activation of JAK1/3 and spleen tyrosine kinase (SYK) in primary cultured podocytes. IL-15-dependent JAK/SYK induction was impaired in the absence of γ C or IL-2R β . Given that we found γ C largely induced on podocytes during human glomerulonephritis, we propose that renal lesions are indeed modulated by intrinsic glomerular cells through the γ C/IL-2R β receptor response, to date classically described only in immune cells.

Keywords: glomerulonephritis, γ C chain, lymphocyte, podocyte, IL-2R β , IL-15

Introduction

Human crescentic glomerulonephritis (CG) and rapidly progressive glomerulonephritis (RPGN) are life threatening immune-mediated diseases¹. For many years, the pathogenesis of human RPGN has been studied using the experimental model of passive anti-glomerular basement membrane glomerulonephritis (anti-GBM-GN) whereby heterologous anti-glomerular basement membrane (GBM) serum is injected into rats or mice². Following injection, there is a strong inflammatory response, which in a few days leads to severe glomerular and tubulo-interstitial injuries^{3,4}: renal cells become surrounded by lymphocytes, a feature reminiscent of human CG⁵⁻¹⁰. The development of anti-GBM-GN lesions in mice has been shown to involve a CD4⁺ T cell response through either Th1^{4,11-14} or Th17¹⁵⁻¹⁷ pathways, while the T cell subset of invariant natural killer T (iNKT) cells exerts a protective role independently of T cell polarization¹⁸.

Interestingly, other studies have reported that mice or rats born athymic or “nude”, i.e. constitutively lacking T cells, still develop classical features of GN after anti-GBM serum injection, which is hypothesis-generating, and provides an opportunity to explore the particular role potentially played by renal cells, independently from T cells^{19,20}, and by intra-renal signaling pathways or local factors normally used by lymphocytes. We thus induced an experimental glomerulonephritis in several immunodeficient mice strains: *Rag2*^{-/-}, *Rag2*^{-/-}*Il2rg*^{-/-} and *Rag2*^{-/-}*Il2rb*^{-/-} which are devoid of either T/B cells or T/B/NK cells. Compared to *Rag2*^{-/-} mice, *Rag2*^{-/-}*Il2rg*^{-/-} and *Rag2*^{-/-}*Il2rb*^{-/-} strains carry the additional deletion of either the interleukin IL-2 receptor common gamma chain (γ C) gene (*Rag2*^{-/-}*Il2rg*^{-/-}) or the IL-2 receptor β subunit (IL-2R β) gene (*Rag2*^{-/-}*Il2rb*^{-/-}). Several interleukin receptor complexes share the γ C subunit (IL-2, IL-4, IL-7, IL-9, IL-15, and IL-21)²¹. Importantly, IL-15 and IL-2, together with an IL-15R α or IL-2R α co-receptor respectively, have their action further restricted to the β subunit. The trimeric IL-15

receptor (IL-15R α , IL-2R β , γ C) is necessary for NK cell ontogeny and explains the absence of NK cells in *Rag2^{-/-}Il2rg^{-/-}* or *Rag2^{-/-}Il2rb^{-/-}* mice. In this paper we show that γ C/ IL-2R β complexes expressed at the surface of intrinsic renal cells play an important role in the organization of renal lesions during severe immune-mediated glomerulonephritis.

Results

***Rag2^{-/-}Il2rg^{-/-}* mice are more susceptible than *Rag2^{-/-}* mice to anti-GBM serum**

Experiments were first carried out to test the effect of anti-GBM serum in *Rag2^{-/-}* mice devoid of T/B cells, *Rag2^{-/-}Il2rg^{-/-}* mice devoid of T/B/NK cells, and wild type (WT) mice from the same C57BL/6J background. Administration of anti-GBM serum impaired renal function parameters and induced lesions typical of glomerulonephritis in WT, *Rag2^{-/-}* and *Rag2^{-/-}Il2rg^{-/-}* mice (**Figure 1A**) evaluated at day 9. No marked differences were observed in the levels of blood urea nitrogen (BUN) and percentage of pathologic glomeruli between anti-GBM treated WT mice and *Rag2^{-/-}* mice (**Figures 1B & 1C**). However, the score of interstitial lesions, assessed by tubular dilations and epithelial atrophy, was lower in anti-GBM treated *Rag2^{-/-}* mice compared to anti-GBM-GN treated WT mice (**Figure 1D**). The levels of plasma urea, proteinuria and the severity of renal histological lesions were even greater in anti-GBM treated *Rag2^{-/-}Il2rg^{-/-}* mice than in anti-GBM treated *Rag2^{-/-}* mice (**Figure 1B-E**). Anti-GBM-GN treated *Rag2^{-/-}Il2rg^{-/-}* mice consistently exhibited more significant tubulo-interstitial lesions, CD44 de novo staining (**Supplemental Figure 1**), a higher percentage of pathologic glomeruli (**Figures 1C & 1D**) and a more important decrease in the podocytic marker podocalyxin (**Figure 1F**) than anti-GBM treated *Rag2^{-/-}* mice. Therefore, *Rag2^{-/-}* mice appeared only partially protected against anti-GBM-GN, while *Rag2^{-/-}Il2rg^{-/-}* mice were found to be more susceptible to anti-GBM serum than WT or *Rag2^{-/-}* mice.

NK cells have no protective role against renal lesions induced by anti-GBM serum

Rag2^{-/-} mice have been shown to have a significant proportion of circulating NK cells (around 25% vs 5% in WT mice), while *Rag2^{-/-}Il2rg^{-/-}* mice totally lack NK cells²². To determine the role of NK cells in the results shown above, *Rag2^{-/-}Il2rg^{-/-}* mice were replenished by NK cells (1×10^6

cells/mouse), isolated from the spleen of WT C57BL/6J mice, and injected together with anti-GBM serum. At day 7, flow cytometry analysis showed that ~ 2% of circulating cells in *Rag2*^{-/-} *Il2rg*^{-/-} mice were NK cells (**Figure 2A**). At day 9, NK cells were also detected in the mice kidneys (**Figure 2B**), where an increase in mRNA expression of the *Nkg2b/Cd159a* NK cell receptor (**Figure 2C**) was detectable. Despite that, plasma urea levels and renal lesions were similar to non-replenished *Rag2*^{-/-} *Il2rg*^{-/-} mice (**Figures 2D to 2F**). These findings suggest that NK cells do not account for the severity of glomerulonephritis in *Rag2*^{-/-} *Il2rg*^{-/-} mice.

The lack of γ C expression in renal cells worsens renal lesions induced by anti-GBM serum

Using bone marrow graft experiments we then analyzed the role of kidney-expressed γ C in the development of renal lesions in anti-GBM-GN. Bone marrow cells isolated from WT or *Rag2*^{-/-} CD45.1⁺ mice were grafted into irradiated *Rag2*^{-/-} *Il2rg*^{-/-} CD45.2⁺ (referred to as ep. γ c^{-/-}) mice, in order to obtain chimeric mice knockout only for the γ C chain in non-immune cells. Six weeks after bone marrow transplantation at least 90% of circulating cells expressed the CD45.1⁺ marker in *Rag2*^{-/-} *Il2rg*^{-/-} CD45.2⁺ recipients (**Supplemental Figure 2A**). NK cell counts measured after bone marrow transplantation are represented in **Supplemental Figure 2B**. In all anti-GBM-GN induced ep. γ c^{-/-} chimeric mice, plasma urea levels were consistently higher than in mice with WT epithelia (**Figure 3A**). All ep. γ c^{-/-} chimeric mice exhibited significantly severe glomerular lesions with numerous extra-capillary crescents (**Figures 3B and 3E**) and proteinuria (**Figure 3D**). In addition, the tubulo-interstitial lesions were more severe in ep. γ c^{-/-} mice than in mice with WT epithelia, independent of the origin of the bone marrow (WT or *Rag2*^{-/-}) (**Figures 3C and 3E**). These findings suggest that γ C expressed on renal cells plays a protective role during anti-GBM-GN.

Despite the absence of lymphocytes, IL-15 appears as the main effective ligand of γ C in the renal cortex during glomerulonephritis

We next analyzed relative expression levels of cytokines (*e.g.* IL-2, IL-4, IL-7, IL-9, IL-15, and IL-21) acting through receptor complexes containing the common γ C subunit in the renal cortex of WT, *Rag2*^{-/-} or *Rag2*^{-/-}*γC*^{-/-} mice (**Figure 4A**) after anti-GBM-GN. In all cases, IL-21 and IL-4 mRNA were undetectable. The level of IL-2 mRNA remained very low in all mouse strains (**Figure 4A**). IL-7 and IL-9 mRNA were detectable in the renal cortex, but no difference was observed between WT, *Rag2*^{-/-}, or *Rag2*^{-/-}*Il2rg*^{-/-} mice. Interestingly, IL-15 mRNA was found to be highly expressed in the renal cortex after anti-GBM-GN in the absence of T/B lymphocytes (*Rag2*^{-/-} mice) or even in the absence of T/B/NK cells in *Rag2*^{-/-}*Il2rg*^{-/-} animals (**Figure 4A**). Thus, and as described by others²³, IL-15 is abundantly produced by intrinsic renal cells, which we confirmed by immunohistochemistry of the renal cortex (**Figure 4B**). We also showed that from cytokines classically associated with the γ C response, only IL-15 plasma levels were found to be higher in *Rag2*^{-/-}*Il2rg*^{-/-} mice compared to WT animals (**Supplemental Figure 3A**). To explore the role of IL-15, we challenged *Rag2*^{-/-}*Il15*^{-/-} and *Rag2*^{-/-} littermates with anti-GBM serum: plasma urea and proteinuria were found to be higher in *Rag2*^{-/-}*Il15*^{-/-} mice compared to *Rag2*^{-/-} mice (**Supplemental Figures 4 A, B, C**). Next, we induced an anti-GBM-GN in *Rag2*^{-/-}*Il2rb*^{-/-} mice lacking the γ C co-receptor IL-2R β . Again, *Rag2*^{-/-}*Il2rb*^{-/-} mice were found to be highly sensitive to anti-GBM serum when compared to *Rag2*^{-/-} mice. Both strains developed acute renal failure, yet plasma urea levels (**Figure 4C**), tubulo-interstitial lesions (**Figures 4E/G**) and proteinuria (**Figure 4F**) were significantly greater in *Rag2*^{-/-}*Il2rb*^{-/-} than in *Rag2*^{-/-} mice

(**Figure 4D**). Taken together, these results suggest that in the absence of lymphocytes, IL-15 and its co-receptors γ C and IL-2R β have a protective role during anti-GBM-GN.

IL-15R α , γ C and IL-2R β receptor subunits are expressed in renal cells during anti-GBM-GN

Immunohistochemical studies evidenced noticeable intra-renal expression of γ C and its co-receptor complexes, IL-2R β and IL-15R α . Interestingly, γ C and IL-15 co-receptors IL-15R α and IL-2R β were not expressed at the basal state in glomeruli. Nevertheless, they are induced during anti-GBM-GN (**Figures 5A to C**). Co-localization studies in *Rag2*^{-/-} mice showed that γ C is mainly induced in podocytes during anti-GBM-GN (**Figure 5D**). These findings indicate that γ C, IL-2R β and IL-15R α are expressed in renal epithelium and in particular by injured glomeruli during anti-GBM-GN. We also demonstrated the presence of IL15R α and IL2R β proteins from the renal cortex by immunoblot (**Supplemental Figure 3B**). These receptors were not kidney-specific *Il2rg* (γ C) or *Il2rb* splice variants. In particular, RNA-Seq analysis revealed that all “classical” transcripts and exons of γ C, originally described in lymphocytes, are expressed in the kidneys of *Rag2*^{-/-} mice (**Supplemental Figures 5 A, B, C**).

Renal epithelial IL-15 signaling is impaired in the absence of γ C or IL-2R β

In vitro experiments were carried out on primary cultured podocytes in which γ C has been demonstrated to be highly expressed. Mice primary podocytes from the *Rag2*^{-/-}*Il2rb*^{-/-}, *Rag2*^{-/-}*Il2rg*^{-/-} or WT kidney cortex were cultivated from glomerular extracts and stimulated by IL-15 (**Figure 6A**). The purity of glomerular extracts was also confirmed by microscopy (**Figure 6B**). To confirm the functionality of IL-15 receptors we studied downstream effectors classically

known in lymphocytes: phosphorylated JAK 1/3 and spleen tyrosine kinase (SYK). As described in immune cells, IL-15 induced JAK1/3 and SYK phosphorylation in primary cultured podocytes (**Figures 6A/C/D/E**). However, despite the absence of γ C, JAK1/3 was still induced in primary podocytes from *Rag2^{-/-}Il2rg^{-/-}* mice (**Figures 6A/C/D**), while SYK phosphorylation dramatically decreased (**Figures 6A and 6E**). There was no JAK and SYK phosphorylation in the absence of IL-2R β (**Figures 6A/C/D/E**). Thus, IL-15 signaling on primary podocytes appears to be more dependent on IL-2R β than on γ C.

Common γ chain is also induced in human podocytes during glomerulonephritis

We finally analyzed the expression of γ C on human renal biopsies from patients with crescentic glomerulonephritis, using pristine 3-month post-transplant renal biopsies as controls. Interestingly, γ C was weakly expressed in control biopsies, but was largely induced in glomeruli during glomerulonephritis. Despite being weaker than in its severe form, the expression of γ C appears at the early stage of glomerulonephritis and is visible on fibrotic glomerular lesions (**Figure 7A**). We determined that γ C was expressed by human podocytes during glomerulonephritis, indeed γ C co-localized with nephrin and synaptopodin (**Figure 7B**). These results suggest that γ C could be an early danger signal expressed by podocytes during glomerulonephritis.

Discussion

Previous studies have described the role of immune cells during the development of renal injury in the passive experimental model of anti-GBM-GN^{4,13,17,24,25}. To date, many studies support a central role for T lymphocytes in the generation of renal lesions^{4,26}. Because renal lesions are observed despite the absence of B and T lymphocytes in mice, we propose that intrinsic renal cells play a central role in the development of anti-GBM-GN²⁷⁻³⁰. Our findings are also in agreement with those of earlier studies that evaluated passive anti-GBM-GN lesions in nude animals^{19,20}. Similar observations regarding glomerular injury in the absence of T cells were also made in *Rag1*^{-/-} mice in another experimental model (Alport's Syndrome) in which inflammatory cells are believed to contribute to renal lesions. In this latter study, T cells were not required for the emergence of glomerular injury, but may have contributed to the development of tubular lesions³¹. In our study we find similar results in the passive anti-GBM-GN model, as tubulo-interstitial lesions appear less severe in *Rag2*^{-/-} mice compared to those observed in WT mice.

When re-examining the role of T lymphocytes during the generation of anti-GBM-GN lesions it appears that several points could in fact reconcile our findings with previous studies.

First, active and passive experimental anti-GBM-GN models are often unintentionally scrambled. The passive form, used in our study, results from the injection of a heterologous anti-GBM serum, whereas the active model is the result of the “active” immunization of the host against glomerular extracts or specific GBM epitopes breaking self-tolerance³²⁻³⁴. The active model is largely dependent on cell-mediated immunity (CMI) whilst our work demonstrates that the passive model is not dependent in this way. Second, the very first studies demonstrating the role of CMI during passive anti-GBM-GN were made using either depleting antibodies, with

potential off-target effects, or an unstable genetic background³⁵⁻³⁸. Third, some passive-anti-GBM-GN phenotypes, acquired in mutant mice engineered with defective CMI effectors, could be explained by a defect in renal cells *per se* or the unsuspected direct action of immunosuppressive drugs on renal epithelial cells³⁹. This defect in intra renal CMI effectors would be evident only during the disease state and has been observed in STAT3 or B7-1 knock out animals. STAT3 signaling has been shown to be engaged in the immune process and during experimental anti-GBM-GN⁴⁰. B7-1/CD80 was first demonstrated to be an important CMI effector expressed on immune cells acting as costimulatory molecules. Later, B7-1 was found expressed on podocytes and regulating the filtration barrier in immune-mediated kidney diseases⁴¹. Our work also illustrates this point. Indeed, we demonstrate that γ C plays an important role in epithelial cells only during glomerulonephritis.

Using double knockout animals (*Rag2^{-/-}Il2rg^{-/-}*) and bone marrow graft experiments, we demonstrate that the expression of γ C in the kidney plays a major role in the development of passive anti-GBM-GN. To our knowledge ours is the first study to show a role of a tissue-expressed γ C chain. This result is obtained in the absence of lymphocytes. Several interleukin receptor complexes (IL-2, IL-4, IL-7, IL-9, IL-15, and IL-21) share the γ C subunit²¹. As with γ C, IL-2R β is also part of the co-receptor complex that signals only for IL-2 and IL-15⁴². But IL-2 or IL-15 signaling requires an additional α subunit leading to functional receptor complexes formed with IL-2R α /IL-2R β / γ , or IL-15R α /IL-2R β / γ . To date, γ C or IL-2R β expressions have been reported in primary cultured tubular epithelial cells or renal tumoral cells but not in glomerular cells (*e.g.* endothelial, mesangial or even visceral epithelial cells) in mice or humans^{43,44}.

Given either their absence or very low level of expression during anti-GBM-GN, we did not consider that IL-2, IL-4, IL-7, IL-9 – or even IL-21 – played an important role during anti-

GBM-GN. These results and the severity of the anti-GBM-GN observed in *Rag2^{-/-}Il2rb^{-/-}* mice pointed to IL-15 in particular. We demonstrate that IL-15 *per se* confers a powerful protective effect against anti-GBM-GN in the absence of lymphocytes. These results are partially in line with the original study by Shinozaki *et al.*²³ Using *Il15^{-/-}* mice in the same model, this study demonstrated that IL-15 produces an important anti-apoptotic effect in epithelial cells. However, as opposed to the hypothesis of Shinozaki *et al*, our study highlights that the IL-15 epithelial protective effect appears marginally T cell driven.

Our *in vitro* data suggest that podocytes use the classical IL-15/JAK/SYK signaling pathways described in immune cells^{21,43-46}. Impaired JAK/SYK activation on epithelial cells could therefore explain the severe renal lesions in mice lacking γ C or IL-2R β compared to their WT counterparts. Some publications suggest a role for SYK during glomerulonephritis^{47,48}. Despite the absence of γ C, IL-15 unexpectedly induces JAK phosphorylation. We hypothesize that IL-2R β dimerization could occur in the absence of γ C but yet still lead to JAKs phosphorylation and thus permit beneficial IL-15 downstream events. Inhibition of SYK with a non-selective SYK inhibitor (fostamatinib) has been shown to confer protection in WKY rats, both during nephrotoxic nephritis⁴⁷ and experimental autoimmune nephritis⁴⁹. One of the hypotheses put forward in these papers has been the reduction of SYK activity following Fc gamma Receptor I and III activation. In both studies we cannot exclude the possibility that, in spite of serious SYK inhibition, IL-15 levels have been augmented by favorable off-target effects. Moreover, given its action on FLT3, JAK, LCK and c-Kit⁵⁰, fostamatinib appears as a non-specific inhibitor of SYK, limiting its value. Thus, according to these data, it is hard to reconcile our findings with previous works, given that IL-15 levels were not evaluated coupled with the pleiotropic effects of SYK. Moreover, our results show that IL-15 induces a protecting signal by

activating SYK in the epithelium. We think that global inhibition could affect both immune cells and the epithelium which play different roles in shared SYK signaling. Further studies are required in order to analyze the nature of SYK-associated epithelial signaling.

All these findings contribute to our understanding of epithelial-specific IL-15 signaling and suggest that γ C and IL-2R β may modulate different downstream survival events. IL-2R β /JAK interactions have been studied mainly *in vitro* as part of the IL-2 response rather than that of IL-15⁵¹. Similar to the observed effects in anti-GBM-GN-induced renal lesions, IL-2/IL-15 receptors have been reported to be a key anti-apoptotic factor in both immune and epithelial mammary cells⁵². Altogether, the intra-renal expression of IL-15 signaling may represent a key functional *modus operandi* that limits epithelial lesions associated with glomerulonephritis. These effects may be related to STAT5 action or to other signaling proteins such as SYK which are involved in the IL-15 response^{53,54}. Further studies are needed to determine more precisely the intra-renal role of downstream IL-15 signaling effector events in the model of anti-GBM-GN.

NK cells are notably expanded in *Rag2*^{-/-} animals and have been shown to produce large amounts of IL-15⁵⁵, which may lead to some beneficial effects, in tubular cells in particular. This might explain why *Rag2*^{-/-} mice present fewer tubulo-interstitial injuries than their WT counterparts. But the effect, if any, should be local and dependent on IL-2R β . Indeed, the reintroduction of NK cells in *Rag2*^{-/-}*Il2rg*^{-/-} mice was insufficient to protect them against anti-GBM serum in glomeruli but seems to have a protective effect in tubular cells in which only IL-2R β could have relayed the IL-15 signal. Similarly, in *Rag2*^{-/-} animals, we cannot exclude a possible role for innate lymphoid cells (ILC) which might afford protection by promoting IL-15 production in NK cells as hypothesized above. Further studies are needed to specifically address these questions.

In conclusion we demonstrated that significant renal lesions occur in the absence of T and B or even NK cells during experimental passive anti-GBM-GN. We also showed that epithelial-expressed immune receptors such as γC and its IL-2R β co-receptor can largely modulate the protective effect of IL-15, an interleukin which is highly expressed by the kidney epithelium. We also confirmed that human podocytes express γC during glomerulonephritis suggesting that renal-expressed immune receptors such as $\gamma C/IL-2R\beta$ *per se* might represent unsuspected targets during glomerulonephritis.

Methods

Animals

C57BL/6J WT mice were obtained from the Charles Rivers Laboratory (L'Arbresle, France). C57BL/6J *Rag2*^{-/-}*Il2rg*^{-/-}CD45.1 mice were kindly provided by S. Ezine and F.Vasseur (Inserm U1020, Paris, France). C57BL/6J *Rag2*^{-/-}CD45.2 mice and *Rag2*^{-/-}*Il2rg*^{-/-} mice were provided by J.C. Bories (Centre Hayem EA 3963, Paris, France). C57BL6J *Rag2*^{-/-}*Il2rb*^{-/-} mice and *Rag2*^{-/-}*Il15*^{-/-} mice were provided by J. Di Santo (Institut Pasteur, Paris, France). Description of the immunological phenotypic of these different mice strains has been previously described^{55,56}. Mice submitted to sanitary control tests to ensure proper pathogen-free status were housed in the same animal facility before any experiments. All mice were backcrossed at least 12 times into a C57BL/6J background to ensure a similar genetic background. We provide body weights and basal renal phenotypes in **Supplemental Table 1**. All mice were held in the same SPF conditions during breeding.

Experimental anti-GBM glomerulonephritis

Passive experimental anti-GBM-GN was induced using de complemented sheep anti-rat GBM serum prepared as previously described¹⁸. Passive non-accelerated anti-GBM-GN was induced by daily intravenous administration of 1.5 mg total protein/ g body weight for three consecutive days as previously described³. Renal injury was evaluated on day 9 following the last injection of anti-GBM serum. As controls, mice were injected with phosphate buffered saline (PBS) or normal sheep serum. BUN, urinary protein and creatinine levels were measured using a Konelab enzymatic-spectrophotometric analyzer (Thermo Scientific).

NK cells isolation and transfer in *Rag2*^{-/-}*Il2rg*^{-/-} mice

NK cells were isolated from C57BL/6J WT mice spleen cell suspension using the NK Cell Isolation Kit, an LS Column, and a MidiMACS™ Separator according to the manufacturer's instructions (Miltenyi Biotec). The NK cells were then injected intravenously (1×10^6 cells in 100 μ l in sterile PBS per mouse) to *Rag2^{-/-}Il2rg^{-/-}* mice.

Bone marrow transplantation

CD45.2⁺ WT C57BL/6J mice and *Rag2^{-/-}Il2rg^{-/-}* mice were X irradiated (700 rad/mouse) to deplete bone marrow progenitors, and then reconstituted 24 h later by intravenous retro-orbital injection of 10×10^6 bone marrow white cells obtained from flushed femurs and tibias derived from donor CD45.1⁺ mice. Mice were then left for six weeks for bone marrow reconstitution.

Histological and immunohistochemical studies

Kidneys were fixed in formalin solution (4%), and embedded in paraffin. Sections (4- μ m thick) were stained by Masson's trichrome to determine proportion of positive glomeruli which were defined by crescent formation (defined as glomeruli exhibiting ≥ 2 layers of cells in Bowman's space, with or without podocyte injury, as indicated by ballooning, necrosis, or cyst formation) and/or fibrin deposition. The proportion of glomeruli affected was determined by a blinded examination on at least 50 glomeruli per section. Tubular lesions were evaluated semi-quantitatively as follows: 0, no tubular dilation; 1, dilation in 1–25% of the tubules analyzed; 2, dilation in 26–50% of the tubules analyzed; 3, dilation in 51–75% of the tubules analyzed; 4, dilation in >76% the tubules analyzed.

Immunohistochemical studies were performed on dewaxed kidney 4- μ m sections which were incubated for 30 minutes at 95°C in the target retrieval solution (Dako), then in peroxidase blocking reagent (Dako), blocked in PBS containing 5% BSA and immunostained against IL-15 (R&D Systems), γ C (Biolegend), IL-2R β (Novus Biologicals), IL-15R α (Novus Biologicals),

CD44 (Abcam) and podocalyxin (R&D Systems). Specific staining was revealed using Histofine reagents, which contained anti-rabbit or anti-rat immune-peroxidase polymer.

For NK cell and IL-2R γ c stainings, 4- μ m kidney cryosections were blocked with 5% BSA-PBS for 10 minutes at room temperature. Kidney sections were then incubated with anti-Ly49G2 (BD Biosciences Pharmingen) or anti-IL-2R γ c (Biolegend) antibodies overnight. For Ly49G2 staining kidney sections were then incubated sequentially with biotinylated secondary antibody, avidin-biotin-peroxidase complex (ABC-Elite; Vector Laboratories), and 3,3'-diaminobenzidine (with nickel chloride enhancement). For IL2R γ c specific staining was revealed using Histofine anti-rat secondary antibody and AEC (Dako). Images were obtained with optical microscopy (Olympus, Hamburg, Germany).

Immunofluorescence assay and confocal microscopy

Rabbit anti-IL2R γ c (Biolegend), rabbit anti-synaptopodin (Santa Cruz) and rabbit anti-nephrin (LifeSpan BioSciences Inc.) antibodies were incubated overnight on frozen kidney slides after blocking with PBS containing 5% BSA. Kidney sections or human tissues were then incubated with anti-rat Alexa Fluor 488, or anti-rabbit Alexa Fluor 546 conjugated secondary antibodies (Invitrogen). The nuclei were stained using DAPI (Invitrogen). Images from mice tissues were obtained with laser scanning confocal microscopy (TCS SP2 AOBS, Leica, Wetzlar, Germany). Acquisition software used was Leica Confocal Software and images (x630) were processed using Image J®. Images from human tissues were obtained with a wide-field light microscope (IX83, Olympus) and processed using Image J®.

Flow cytometry

Blood samples (50 μ l) from mice were incubated for 1 h at 4°C with anti-mouse CD45.1, CD45.2 or Ly49G2 primary antibodies or corresponding isotype controls (BD Biosciences Pharmingen). After washing, cells were then incubated with alexa488-coupled anti-rat IgG (Invitrogen) for 30

min at 4°C. Red cells were then lysed and resuspended cells were analyzed using a FACScanto II flow cytometer (BD Biosciences Pharmingen).

Quantitative RT-PCR

RNA was extracted from whole kidneys using TRIzol solution (Life Technologies). Residual genomic DNA was removed by DNase I treatment (Fermentas). RNA samples (1 μ g) were reverse-transcribed using a Revert Aid H minus First Strand DNA Synthesis kit (Fermentas). *Beta-Glucuronidase (Gusb)* and *Hypoxanthine-guanine phosphoribosyltransferase (Hprt1)* genes were used as endogenous reference housekeeping genes. The specific PCR primer sequences used are listed in **Supplemental Table 2**. Normalization of the quantitative PCR (qPCR) data PCR analysis obtained using a LightCycler 480 (Roche Diagnostics) was performed using the Roche LightCycler 2.0 software (Roche Diagnostics). Data were expressed as 2^{-DCp} , where Cp corresponds to the cycle threshold number.

In vitro assays in cultured podocytes

Freshly isolated renal cortex from *WT*, *Rag2^{-/-}Il2rg^{-/-}* or *Rag2^{-/-}Il2rb^{-/-}* mice were mixed and digested by collagenase I (1 mg/ml; Gibco) in RPMI 1640 (Gibco) for 2 minutes at 37°C. Next, collagenase I was inactivated with RPMI 1640 plus 10% FBS (Hyclone). Tissues were then passed through a 100- μ m cell strainer and a 40- μ m cell strainer (BD Falcon) in PBS (Euromedex) with 0.5% BSA (Euromedex). Glomeruli, adherent to the 40- μ m cell strainer, were removed from the cell strainer with PBS with 0.5% BSA injected under pressure, and finally washed twice in PBS. Freshly isolated glomeruli purity was analyzed by light microscopy (**Figure 6B**) and then were plated in six-well dishes in RPMI 1640 with 10% FBS, 2% HEPES buffer (Gibco), and 1% penicillin/streptomycin (Gibco). Two days after seeding, glomeruli became adherent to the dish, and podocytes spread out from glomeruli.

Primary podocytes were cultured on RPMI 1640 with 1% FBS for 12 hours and then stimulated 7 days after seeding with mouse recombinant IL-15 (ref. PMP47, Bio-Rad AbD Serotec), at 50

ng/ml for 30 minutes and then mixed in RIPA buffer (Santa Cruz) with orthovanadate, PMSF, protease inhibitor cocktail (Santa Cruz) and NaF and frozen at -80°C for protein extraction.

Western blot analysis from cultured primary podocytes

After extraction from podocytes with lysis buffer, samples were fractionated by SDS-PAGE NuPAGE 4/12% gels (Invitrogen) under reducing conditions and then transferred to a polyvinylidene difluoride membrane. Membranes were incubated with the appropriate primary antibodies: anti-phosphorylated JAK1 (Cell Signaling), JAK3 (Cell Signaling), SYK (Novus Biologicals), anti-IL15R α (Novus Biologicals), anti-IL2R β (Novus Biologicals). Protein loading was monitored by using the rabbit anti-GAPDH antibody (Sigma). Secondary antibody was horseradish peroxidase-conjugated goat anti-rabbit or anti-rat IgG (Amersham). Antigens were revealed with enhanced chemiluminescence (ECL)-plus (Amersham) on autoradiography films (Fuji). Relative quantification was made using Image J[®] software.

Plasma cytokine measurement

Frozen plasma from WT, *Rag2*^{-/-} and *Rag2*^{-/-}*Il2rg*^{-/-} mice were collected at day 9 following anti-GBM-GN induction. γC -associated cytokine plasma levels were measured using a ProcartaPlex Mix&Match Mouse 6-Plex (Ebioscience SAS, Affimetrix) according to the manufacturer's protocol.

Human tissues

Frozen renal biopsy specimens were obtained from the Hôpital Tenon, Assistance Publique-Hôpitaux de Paris, Paris, France, according to local procedures. Only renal biopsy specimens with a sufficient amount of tissue remaining after completion of diagnostic workup were included for immunohistochemical evaluation.

High throughput RNA-Sequencing, demonstration of absence of specific kidney splice variants

RNA samples from non-nephritic kidneys from *Rag2*^{-/-} (and *Rag2*^{-/-}*Il2rg*^{-/-} kidney cortex as a negative control) (n=2 per group) of high quality (RNA Integrity Number >6) were processed to create a mRNA library using TrueSeq reagents (Illumina). Clusters were created for Illumina RNA-Sequencing using a CBot system and sequencing was carried out on one lane of HiSeq2000 to produce paired-end reads (75 bases length, 29 to 35 million of reads per sample). After demultiplexing, bar-coding removal, quality control and paired-end reads were processed from Fastq Sanger format to compact-reads format and then aligned with STAR (default parameters) to the mouse reference genome (mGC37/mm9) in order to seek putative kidney specific splice variants. Data alignment and analysis were performed using the GobyWeb interface and examined visually at the *Il2rg* locus in the Integrative Genomic Viewer (<http://www.broadinstitute.org/igv/>) respective of Ensembl Annotation (Ensembl version 55).

Statistics

Values are given as means \pm SEM. Statistical analysis was performed using the GraphPad Prism program. The Mann-Whitney test was used to compare two groups. Kruskal-Wallis test analyzed the distribution of three or more groups. A p value < 0.05 was considered significant.

Study approval

All mouse studies were submitted to, and approved by, the French Institutional Animal Care and Use Committee (Hôpital Tenon, AP-HP, Paris, France) and the Ethics Committee Charles Darwin (Paris, France) (ref n° 5 ECCD).

Disclosures

The authors have declared that no conflict of interest exists.

References

1. Couser WG. Rapidly progressive glomerulonephritis: classification, pathogenetic mechanisms, and therapy. *Am. J. Kidney Dis. Off. J. Natl. Kidney Found.* 1988; **11**: 449–464.
2. El Nahas AM. Masugi nephritis: a model for all seasons. In: *Experimental and Genetic Rat Models of Chronic Renal Failure*. editor Karger, Basel, 1993, pp.49–67.
3. Salant DJ, Cybulsky AV. Experimental glomerulonephritis. *Methods Enzymol.* 1988; **162**: 421–461.
4. Tipping PG, Holdsworth SR. T cells in crescentic glomerulonephritis. *J. Am. Soc. Nephrol. JASN* 2006; **17**: 1253–1263.
5. Bohle A, Mackensen-Haen S, von Gise H *et al.* The consequences of tubulo-interstitial changes for renal function in glomerulopathies. A morphometric and cytological analysis. *Pathol. Res. Pract.* 1990; **186**: 135–144.
6. Kriz W, Elger M, Hosser H *et al.* How does podocyte damage result in tubular damage? *Kidney Blood Press. Res.* 1999; **22**: 26–36.
7. Kriz W, LeHir M. Pathways to nephron loss starting from glomerular diseases-insights from animal models. *Kidney Int.* 2005; **67**: 404–419.
8. Rodríguez-Iturbe B, García García G. The role of tubulointerstitial inflammation in the progression of chronic renal failure. *Nephron Clin. Pract.* 2010; **116**: c81-88.
9. Sánchez-Lozada LG, Tapia E, Johnson RJ *et al.* Glomerular hemodynamic changes associated with arteriolar lesions and tubulointerstitial inflammation. *Kidney Int. Suppl.* 2003: S9-14.
10. Scholz J, Lukacs-Kornek V, Engel DR *et al.* Renal dendritic cells stimulate IL-10 production and attenuate nephrotoxic nephritis. *J. Am. Soc. Nephrol. JASN* 2008; **19**: 527–537.
11. Kitching AR, Holdsworth SR, Tipping PG. Crescentic glomerulonephritis--a manifestation of a nephritogenic Th1 response? *Histol. Histopathol.* 2000; **15**: 993–1003.
12. Kitching AR, Tipping PG, Timoshanko JR *et al.* Endogenous interleukin-10 regulates Th1 responses that induce crescentic glomerulonephritis. *Kidney Int.* 2000; **57**: 518–525.
13. Kitching AR, Turner AL, Wilson GRA *et al.* IL-12p40 and IL-18 in crescentic glomerulonephritis: IL-12p40 is the key Th1-defining cytokine chain, whereas IL-18 promotes local inflammation and leukocyte recruitment. *J. Am. Soc. Nephrol. JASN* 2005; **16**: 2023–2033.
14. Tipping PG, Kitching AR. Glomerulonephritis, Th1 and Th2: what's new? *Clin. Exp. Immunol.* 2005; **142**: 207–215.
15. Paust H-J, Turner J-E, Steinmetz OM *et al.* The IL-23/Th17 axis contributes to renal injury in experimental glomerulonephritis. *J. Am. Soc. Nephrol. JASN* 2009; **20**: 969–979.

16. Steinmetz OM, Summers SA, Gan P-Y *et al.* The Th17-defining transcription factor ROR γ t promotes glomerulonephritis. *J. Am. Soc. Nephrol. JASN* 2011; **22**: 472–483.
17. Turner J-E, Krebs C, Tittel AP *et al.* IL-17A production by renal $\gamma\delta$ T cells promotes kidney injury in crescentic GN. *J. Am. Soc. Nephrol. JASN* 2012; **23**: 1486–1495.
18. Mesnard L, Keller AC, Michel M-L *et al.* Invariant natural killer T cells and TGF-beta attenuate anti-GBM glomerulonephritis. *J. Am. Soc. Nephrol. JASN* 2009; **20**: 1282–1292.
19. Kusuyama Y, Nishihara T, Saito K. Nephrotoxic nephritis in nude mice. *Clin. Exp. Immunol.* 1981; **46**: 20–26.
20. Sato T, Oite T, Nagase M *et al.* Nephrotoxic serum nephritis in nude rats: the roles of host immune reactions. *Clin. Exp. Immunol.* 1991; **84**: 139–144.
21. Ring AM, Lin J-X, Feng D *et al.* Mechanistic and structural insight into the functional dichotomy between IL-2 and IL-15. *Nat. Immunol.* 2012; **13**: 1187–1195.
22. Shinkai Y, Rathbun G, Lam KP *et al.* RAG-2-deficient mice lack mature lymphocytes owing to inability to initiate V(D)J rearrangement. *Cell* 1992; **68**: 855–867.
23. Shinozaki M. IL-15, a survival factor for kidney epithelial cells, counteracts apoptosis and inflammation during nephritis. *J. Clin. Invest.* 2002; **109**: 951–960.
24. Holdsworth SR, Kitching AR, Tipping PG. Th1 and Th2 T helper cell subsets affect patterns of injury and outcomes in glomerulonephritis. *Kidney Int.* 1999; **55**: 1198–1216.
25. Kurts C, Heymann F, Lukacs-Kornek V *et al.* Role of T cells and dendritic cells in glomerular immunopathology. *Semin. Immunopathol.* 2007; **29**: 317–335.
26. Tan DSY, Gan PY, O’Sullivan KM *et al.* Thymic deletion and regulatory T cells prevent antimyeloperoxidase GN. *J. Am. Soc. Nephrol. JASN* 2013; **24**: 573–585.
27. Akagi Y, Isaka Y, Arai M *et al.* Inhibition of TGF-beta 1 expression by antisense oligonucleotides suppressed extracellular matrix accumulation in experimental glomerulonephritis. *Kidney Int.* 1996; **50**: 148–155.
28. Couser WG. Basic and translational concepts of immune-mediated glomerular diseases. *J. Am. Soc. Nephrol. JASN* 2012; **23**: 381–399.
29. Huang XR, Tipping PG, Apostolopoulos J *et al.* Mechanisms of T cell-induced glomerular injury in anti-glomerular basement membrane (GBM) glomerulonephritis in rats. *Clin. Exp. Immunol.* 1997; **109**: 134–142.
30. Le Hir M. Histopathology of humorally mediated anti-glomerular basement membrane (GBM) glomerulonephritis in mice. *Nephrol. Dial. Transplant. Off. Publ. Eur. Dial. Transpl. Assoc. - Eur. Ren. Assoc.* 2004; **19**: 1875–1880.

31. Lebleu VS, Sugimoto H, Miller CA *et al.* Lymphocytes are dispensable for glomerulonephritis but required for renal interstitial fibrosis in matrix defect-induced Alport renal disease. *Lab. Investig. J. Tech. Methods Pathol.* 2008; **88**: 284–292.
32. Arends J, Wu J, Borillo J *et al.* T cell epitope mimicry in antiglomerular basement membrane disease. *J. Immunol. Baltim. Md 1950* 2006; **176**: 1252–1258.
33. Reynolds J. Strain differences and the genetic basis of experimental autoimmune anti-glomerular basement membrane glomerulonephritis. *Int. J. Exp. Pathol.* 2011; **92**: 211–217.
34. Steblay RW. Glomerulonephritis induced in sheep by injections of heterologous glomerular basement membrane and Freund's complete adjuvant. *J. Exp. Med.* 1962; **116**: 253–272.
35. Kitching AR, Tipping PG, Huang XR *et al.* Interleukin-4 and interleukin-10 attenuate established crescentic glomerulonephritis in mice. *Kidney Int.* 1997; **52**: 52–59.
36. Kitching AR, Tipping PG, Mutch DA *et al.* Interleukin-4 deficiency enhances Th1 responses and crescentic glomerulonephritis in mice. *Kidney Int.* 1998; **53**: 112–118.
37. Tipping PG, Huang XR, Qi M *et al.* Crescentic glomerulonephritis in CD4- and CD8-deficient mice. Requirement for CD4 but not CD8 cells. *Am. J. Pathol.* 1998; **152**: 1541–1548.
38. Tipping PG, Neale TJ, Holdsworth SR. T lymphocyte participation in antibody-induced experimental glomerulonephritis. *Kidney Int.* 1985; **27**: 530–537.
39. Faul C, Donnelly M, Merscher-Gomez S *et al.* The actin cytoskeleton of kidney podocytes is a direct target of the antiproteinuric effect of cyclosporine A. *Nat. Med.* 2008; **14**: 931–938.
40. Dai Y, Gu L, Yuan W *et al.* Podocyte-specific deletion of signal transducer and activator of transcription 3 attenuates nephrotoxic serum-induced glomerulonephritis. *Kidney Int.* 2013; **84**: 950–961.
41. Reiser J, von Gersdorff G, Loos M *et al.* Induction of B7-1 in podocytes is associated with nephrotic syndrome. *J. Clin. Invest.* 2004; **113**: 1390–1397.
42. Lin JX, Leonard WJ. The role of Stat5a and Stat5b in signaling by IL-2 family cytokines. *Oncogene* 2000; **19**: 2566–2576.
43. Giron-Michel J, Azzi S, Ferrini S *et al.* Interleukin-15 is a major regulator of the cell-microenvironment interactions in human renal homeostasis. *Cytokine Growth Factor Rev.* 2013; **24**: 13–22.
44. Tejman-Yarden N, Zlotnik M, Lewis E *et al.* Renal cells express a functional interleukin-15 receptor. *Nephrol. Dial. Transplant.* 2005; **20**: 516–523.
45. Alves NL, Arosa FA, van Lier RAW. Common gamma chain cytokines: dissidence in the details. *Immunol. Lett.* 2007; **108**: 113–120.

46. Giron-Michel J, Azzi S, Khawam K *et al.* Interleukin-15 Plays a Central Role in Human Kidney Physiology and Cancer through the γc Signaling Pathway. Meurs EF, ed. *PLoS ONE* 2012; **7**: e31624.
47. Smith J, McDaid JP, Bhangal G *et al.* A Spleen Tyrosine Kinase Inhibitor Reduces the Severity of Established Glomerulonephritis. *J. Am. Soc. Nephrol.* 2009; **21**: 231–236.
48. Ryan J, Ma FY, Han Y *et al.* Myeloid cell-mediated renal injury in rapidly progressive glomerulonephritis depends upon spleen tyrosine kinase. *J. Pathol.* 2015.
49. McAdoo SP, Reynolds J, Bhangal G *et al.* Spleen tyrosine kinase inhibition attenuates autoantibody production and reverses experimental autoimmune GN. *J. Am. Soc. Nephrol. JASN* 2014; **25**: 2291–2302.
50. Braselmann S, Taylor V, Zhao H *et al.* R406, an orally available spleen tyrosine kinase inhibitor blocks fc receptor signaling and reduces immune complex-mediated inflammation. *J. Pharmacol. Exp. Ther.* 2006; **319**: 998–1008.
51. Fujii H, Nakagawa Y, Schindler U *et al.* Activation of Stat5 by interleukin 2 requires a carboxyl-terminal region of the interleukin 2 receptor beta chain but is not essential for the proliferative signal transmission. *Proc. Natl. Acad. Sci. U. S. A.* 1995; **92**: 5482–5486.
52. Hughes K, Watson CJ. The spectrum of STAT functions in mammary gland development. *JAK-STAT* 2012; **1**: 151–158.
53. Fehniger TA, Caligiuri MA. Interleukin 15: biology and relevance to human disease. *Blood* 2001; **97**: 14–32.
54. Huntington ND, Legrand N, Alves NL *et al.* IL-15 trans-presentation promotes human NK cell development and differentiation in vivo. *J. Exp. Med.* 2009; **206**: 25–34.
55. Ranson T, Vosshenrich CAJ, Corcuff E *et al.* IL-15 is an essential mediator of peripheral NK-cell homeostasis. *Blood* 2003; **101**: 4887–4893.
56. DiSanto JP, Müller W, Guy-Grand D *et al.* Lymphoid development in mice with a targeted deletion of the interleukin 2 receptor gamma chain. *Proc. Natl. Acad. Sci.* 1995; **92**: 377.

Acknowledgments

This work was supported by Inserm and also in part by the Faculté de Médecine Pierre et Marie Curie (Sorbonne Universités, UPMC Univ Paris 06). Y.L. is a recipient of Fonds d'Etudes et de Recherche du Corps Médical (Assistance Publique des Hôpitaux de Paris), Société Française de Bienfaisance et d'Enseignement de San Sebastian-Donostia, Espagne and Société de Néphrologie grants. D.C. is a recipient of a European Renal Association - European Dialysis and Transplant Association (ERA - EDTA) grant and the support from Agence Nationale de la Recherche (ANR) of France. We thank Edith Bouget, Chloe Cakin and Miftah Madi for their technical assistance, Benedita Rocha and Sophie Ezine (Inserm U1020, Hôpital Necker, Paris, France) for providing *Rag2^{-/-}* CD45.1 and *Rag2^{-/-}Il2rg^{-/-}* CD45.1 mice. We thank Caroline Martin and Claude Kitou for providing animal housing. We thank Enguerran Mouly (Institut Universitaire d'Hématologie, Hôpital St. Louis, Paris, France) for his help during mice irradiation procedures. We thank the Imaging and Cytometry Facility of Tenon, UMR_S 1155 Inserm, Rare and common kidney diseases, matrix remodelling and tissue repair, F-75020, Paris, Sorbonne Universités, UPMC Univ Paris 06, France. We also thank Dr. A Vandewalle (CRI, UMR 1149, Université Denis Diderot – Paris 7, Paris, France) for stimulating discussions.

Figure legends

Figure 1. Mice lacking lymphocytes develop typical lesions of glomerulonephritis following the administration of the anti-glomerular basement membrane (GBM) serum.

(A) Representative images of Masson trichrome stained sections of renal cortex from 8 to 10-week-old wild type (WT), *Rag2*^{-/-} and *Rag2*^{-/-}*Il2rg*^{-/-} mice 9 days after the injection of anti-GBM serum. Lower panels show magnification of glomerular crescentic lesions from upper panels. Scale bar: 50 μ m. (B) Renal function assessed by plasma urea levels at day 9 after the injection of anti-GBM serum. (C & D) Percentage of positive glomeruli presenting crescents and/or fibrin deposition (C), semi-quantitative score of tubular lesions (tubulo-interstitial score or TIS) (D) and proteinuria to creatininuria ratio (E) in untreated 8 to 10-week-old WT mice (n= 5, control [CTL]), and anti-GBM serum-treated 8 to 10-week-old WT mice (n=20), *Rag2*^{-/-} mice (n=15), and *Rag2*^{-/-}*Il2rg*^{-/-} (n=12). Data represent means \pm SEM. *p<0.05. (F) Representative images of podocalyxin staining by immunohistochemistry on kidney sections from 8- to 10-week-old wild type (WT), *Rag2*^{-/-} and *Rag2*^{-/-}*Il2rg*^{-/-} mice at basal state and 9 days after the injection of anti-GBM serum. Scale bar: 50 μ m.

Figure 2. Natural killer (NK) cells are not sufficient to protect *Rag2*^{-/-}*Il2rg*^{-/-} mice from anti-glomerular basement membrane glomerulonephritis (GBM-GN) induced by anti-GBM serum.

(A) Representative dot-plots (3 independent experiments) of NK cell population (in red) evidenced by an anti-Ly49G2 staining (right quadrants) in 10-week-old anti-GBM-GN *Rag2*^{-/-}*Il2rg*^{-/-} mice 7 days after i.v. administration of NK cells isolated from the spleens of wild type (WT) mice (lower right quadrant) or from *Rag2*^{-/-}*Il2rg*^{-/-} mice injected with vehicle alone (upper

right quadrant). **(B)** Representative images of Ly49G2⁺ NK cells staining (arrows) by immunohistochemistry on kidney sections from *Rag2*^{-/-}*Il2rg*^{-/-} mice replenished with NK cells, 9 days after the injection of NK cells (right panel), compared to non-replenished *Rag2*^{-/-}*Il2rg*^{-/-} mice (left panel). Scale bar: 100µm. **(C)** Relative levels of *Nkg2b* mRNA measured by quantitative polymerase chain reaction (PCR) in renal cortex from naïve (control [CTL]) and from anti-GBM-GN WT, *Rag2*^{-/-}, and *Rag2*^{-/-}*Il2rg*^{-/-} mice, which have been replenished (+) or not with NK cells. Data represents means ± SEM from 3 separate kidneys in each condition tested. * p < 0.05 between groups. **(D)** Plasma urea levels (the horizontal bar in the graph represents the mean plasma urea level in C57BL/6J mice at basal state), **(E)** percentage of positive crescentic glomeruli, **(F)** semi-quantitative score of tubulo-interstitial lesions 9 days after injection of anti-GBM serum into 8–10-week-old *Rag2*^{-/-}*Il2rg*^{-/-} mice either replenished (+) or not with NK cells. Values are means ± SEM from 6 mice in each condition tested. In D to F no significant differences were observed between groups.

Figure 3: Tissue common gamma chain (γC) is required to maintain kidney function and renal tissue integrity after anti-glomerular basement membrane (GBM) serum injection.

Bone marrow (BM) cells from 10-week-old wild type (WT) or *Rag2*^{-/-} mice (WT BM or *Rag2*^{-/-} BM, respectively) were transferred into sub-lethally irradiated 10-week-old WT (WT BM => WT, *Rag2*^{-/-} BM => WT) or into *Rag2*^{-/-}*Il2rg*^{-/-} mice (WT BM => *Rag2*^{-/-}*Il2rg*^{-/-}, *Rag2*^{-/-} BM => *Rag2*^{-/-}*Il2rg*^{-/-} mice). **(A to C)** Plasma urea levels (the horizontal bar in the graph represents the mean plasma urea level in C57BL/6J mice at basal state) **(A)**, percentage of crescentic glomeruli **(C)** and semi-quantitative score of tubulo-interstitial lesions **(B)** in chimeric mice (n=5 per group) 9 days after the administration of anti-GBM serum. **(D)** Proteinuria to creatininuria ratio in

chimeric mice (n=5 per group) 4 days after the administration of anti-GBM serum. Values are expressed as means \pm SEM (n=5 per group) and * p < 0.05. **(E)** Representative images of Masson trichrome stained sections of renal cortex from 16-week-old WT or *Rag2^{-/-}Il2rg^{-/-}* mice grafted with WT BM, 9 days after the last injection of anti-GBM serum. Scale bar: 50 μ m.

Figure 4: IL-15 is highly expressed in kidney cortex in a lymphocyte-free environment and its IL-2R β co-receptor deficiency aggravates anti-glomerular basement membrane glomerulonephritis (GBM-GN).

(A) Reverse transcription- polymerase chain reaction (RT-PCR) analysis of common gamma chain (γ C) ligands (IL-2, IL-4, IL-7, IL-9, IL-15, IL-21) mRNA expression in renal cortex homogenates from wild type (WT), *Rag2^{-/-}*, and *Rag2^{-/-}Il2rg^{-/-}* mice analyzed 9 days after anti-GBM serum injection (means \pm SEM of 5 mice per group of two independent experiments). **(B)** Representative image of the expression of IL-15 by immunohistochemistry in *Rag2^{-/-}* and *Rag2^{-/-}Il15^{-/-}* mice as negative controls. Scale bar: 50 μ m. Plasma urea levels in **(C)** (the horizontal bar in the graph represents the mean plasma urea level in C57BL/6J mice at basal state), positive glomeruli **(D)** and semi-quantitative score of tubulo-interstitial lesions **(E)** in 10–12-week-old *Rag2^{-/-}* mice and *Rag2^{-/-}Il2rb^{-/-}* mice, 9 days after the injection of anti-GBM serum. Proteinuria/creatinuria ratios are also expressed in **(F)**. Values are means \pm SEM of 5 10–12-week-old mice per group. **(G)** Representative illustrations of Masson trichrome stained sections of renal cortex from 10–12- week-old anti-GBM-GN-induced *Rag2^{-/-}* and *Rag2^{-/-}Il2rb^{-/-}* mice. Scale bar: 50 μ m.

Figure 5: Expression of IL-15R subunits in the mouse kidney during glomerulonephritis.

Representative images of the expression of IL-15R α (A), IL-2R β (B) or common gamma chain (γ C) (C) by immunohistochemistry in 12-week-old *Rag2*^{-/-} or *Rag2*^{-/-}-glomerular basement membrane (GBM) mice at day 9. Images are representative of at least 5 mice. Scale bar: 50 μ m. IL-15R α has been expressed in some in the tubules during normal conditions, but was largely induced in glomeruli following anti-GBM serum injection. IL-2R β expression was not detected under normal conditions but was observed at day 9 of glomerulonephritis, mainly in glomeruli. The γ C chain expression has been found in glomeruli after anti-glomerular basement membrane glomerulonephritis (GBM-GN). (D) Immunofluorescent staining of nephrin (in red) and γ C chain (in green) on kidney sections from *Rag2*^{-/-} or *Rag2*^{-/-}*Il2rg*^{-/-} mice at day 9 of the anti-GBM-GN. DAPI was used to stain nuclei. The γ C has been found expressed mainly by podocytes. *Rag2*^{-/-} *Il2rg*^{-/-} mice are positive for nephrin (red) but negative for γ C. Representative images from confocal microscopy observations. Scale bar: 50 μ m

Figure 6: Absence of IL2R γ C or IL2R β impairs IL-15 signaling in primary cultured podocytes.

(A) Western blot analysis of phosphorylated JAK1/3 and spleen tyrosine kinase (SYK) proteins from primary cultured podocytes extracted from kidney of 12-week-old wild type (WT), *Rag2*^{-/-} *Il2rg*^{-/-}, *Rag2*^{-/-}*Il2rb*^{-/-} mice. GAPDH was chosen as loading control. (B) Glomerular extracts used for primary podocyte cultures analyzed in light microscopy at 4x magnification (left) and 10x magnification (right). (C, D and E) Ratio of phosphorylated JAK1/3 and SYK on GAPDH is reported with respect to basal conditions using densitometric values from at least 5 mice from each group tested. Values are means \pm SEM* $p < 0.05$ between groups.

Figure 7: γ C is induced in human podocytes during glomerulonephritis

(A) Representative images of the glomerular expression of common gamma chain (γ C) by immunohistochemistry in pristine 3-month post-transplant renal biopsies (2 cases) and in human crescentic glomerulonephritis (4 different cases). (B) Immunofluorescent staining of nephrin or synaptopodin (in green) and γ C chain (in red) on a renal biopsy from a patient with crescentic glomerulonephritis. DAPI was used to stain nuclei. Scale bar: 50 μ m

Supplemental Figure 1: Tubular injury is increased in *Rag2^{-/-}Il2rg^{-/-}* mice kidney during an anti-GBM model

Representative images of CD44 staining by immunohistochemistry on kidney sections from 8- to 10-week-old wild type (WT), *Rag2^{-/-}* and *Rag2^{-/-}Il2rg^{-/-}* mice at basal state and 9 days after the injection of anti-glomerular basement membrane (GBM) serum. Scale bar: 100 μ m

Supplemental Figure 2: Bone marrow graft efficiency evaluation by determination of the CD45.1/(CD45.2+CD45.1) ratio and natural killer (NK) cells counts after bone marrow graft.

Bone marrow (BM) cells from wild type (WT) or *Rag2^{-/-}* mice (WT BM or *Rag2^{-/-}* BM, respectively) were transferred into either sub-lethally irradiated WT (WT BM => WT, *Rag2^{-/-}* BM => WT) or *Rag2^{-/-}Il2rg^{-/-}* mice (WT BM => *Rag2^{-/-}Il2rg^{-/-}*, *Rag2^{-/-}* BM => *Rag2^{-/-}Il2rg^{-/-}* mice). (A) Quantification by flow cytometry of the percentage of circulating CD45.1⁺ cells from the donors over the total CD45⁺ cells and (B) percentage of circulating NK cells over the total CD45⁺ cells in blood from chimeric mice was done at day 9 of the anti-glomerular basement membrane glomerulonephritis (GBM-GN). Values are means \pm SEM (n=5 per group).

Supplemental Figure 3: In the absence of T/B/NK lymphocytes IL-15 is highly produced and its receptors IL15R α and IL2R β are expressed in the renal cortex

(A) Plasma common γ chain dependent cytokine levels at day 9 of anti-glomerular basement membrane glomerulonephritis (GBM-GN) in 10- to 12-week-old wild type (WT), *Rag2*^{-/-} and *Rag2*^{-/-}*Il2rg*^{-/-} mice. Results are expressed as means \pm SEM (5 mice per group). * $p < 0.05$ between groups. (B) Western blot analysis of IL15R α and IL2R β proteins from kidney cortex of 12-week-old WT, *Rag2*^{-/-} and *Rag2*^{-/-}*Il2rg*^{-/-} mice at basal state and at day 9 of anti-glomerular basement membrane glomerulonephritis (GBM-GN) (2 mice per group). GAPDH was chosen as loading control.

Supplemental Figure 4: IL-15 plays a protective role against anti-glomerular basement membrane (GBM) serum in a lymphocyte-free environment.

(A) Plasma urea levels at day 9 (the horizontal bar in the graph represents the mean plasma urea level in C57BL/6J mice at basal state) and (B) protein urinary excretion rate at day 0, day 4 and day 9 of the anti- glomerular basement membrane glomerulonephritis (GBM-GN) in 10 to 12-week-old *Rag2*^{-/-} and *Rag2*^{-/-}*Il15*^{-/-} mice. Results are expressed as means \pm SEM (5 mice per group). (C and D) Representative illustrations of anti-GBM lesions evidenced by Masson's trichrome staining in *Rag2*^{-/-} and *Rag2*^{-/-}*Il15*^{-/-} mice. Scale bar: 50 μ m.

Supplemental Figure 5: Annotated Integrative Genomic viewer (IGV) screenshot focused on the *IL2rg* locus following RNA-Seq analysis from mouse kidney cortex.

Il2rg transcripts according to the Ensembl database (v55) at the *Il2rg* gene locus (GRCm37/mm9). (B and C) Paired-end reads of naïve *Rag2*^{-/-} (B) and *Rag2*^{-/-}*Il2rg*^{-/-} (C) mouse kidneys. All “classical” *Il2rg* exons were represented in the kidney of a *Rag2*^{-/-} mouse, while exons 2 to 7 were absent in the *Rag2*^{-/-}*Il2rg*^{-/-} mouse kidney. Despite numerous transcript variants described in the Ensembl database for *Il2rg* (represented in blue or red in A), exons belonging to

Il2rg were not shared by other proxy genes, such as Gm20489-001 (red on the left in A), excluding any kidney-specific variants with an *Il2rg* similarity. Other processed transcripts, such as *Il2rg*-002 or 003 (blue in A), which do not have a computationally predicted protein coding expression, were not expressed. Conversely, classical transcripts (in red in A, on the right) were expressed at the protein coding level in the kidney of a naïve *Rag2*^{-/-} mouse.

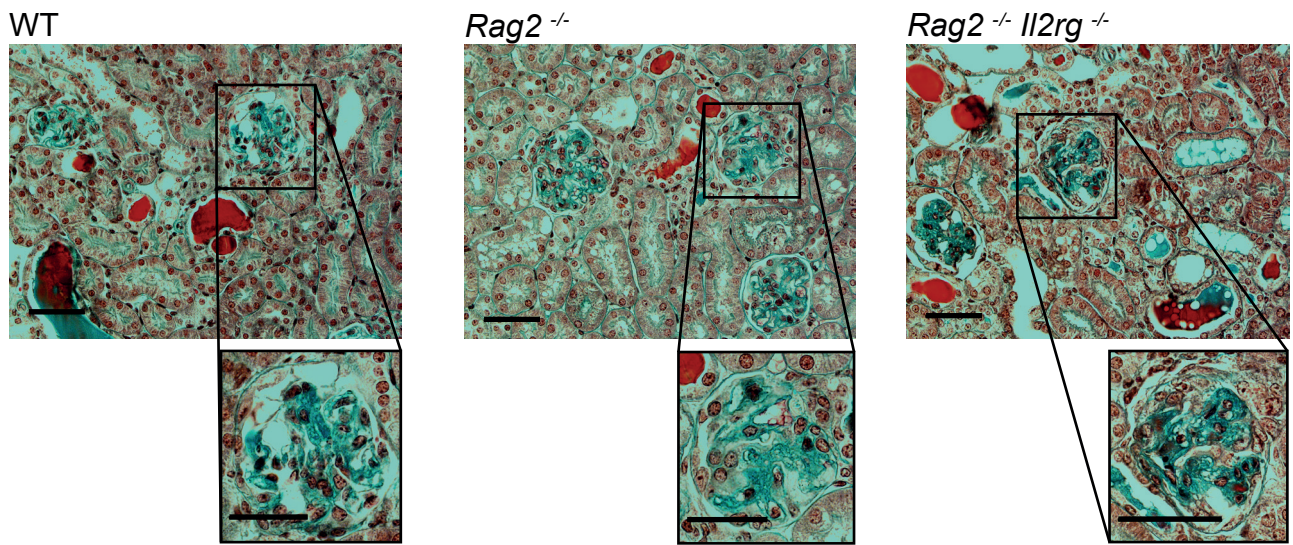
Supplemental Table 1: Basal phenotype of the different immunodeficient mice strains used

Data represents means ± SEM of at least 5 mice per group. Kruskal-Wallis non-parametric test. * p<0.05, ** p<001.

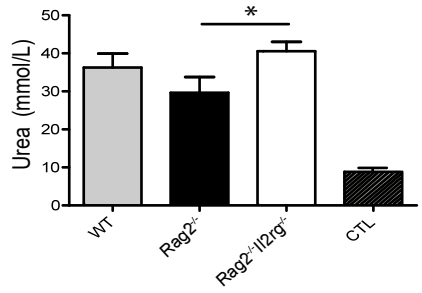
Supplemental Table 2: Polymerase chain reaction (PCR) primer sequences used for quantitative PCR.

Figure 1: Luque et al.

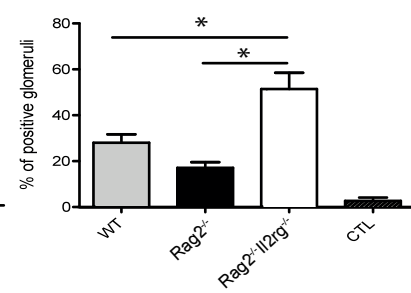
A



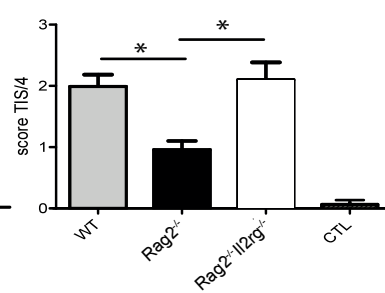
B



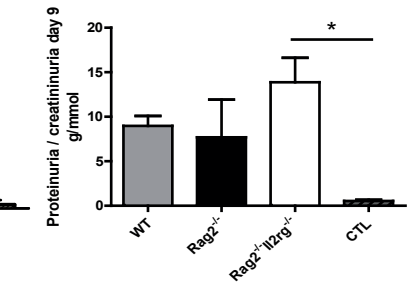
C



D



E



F

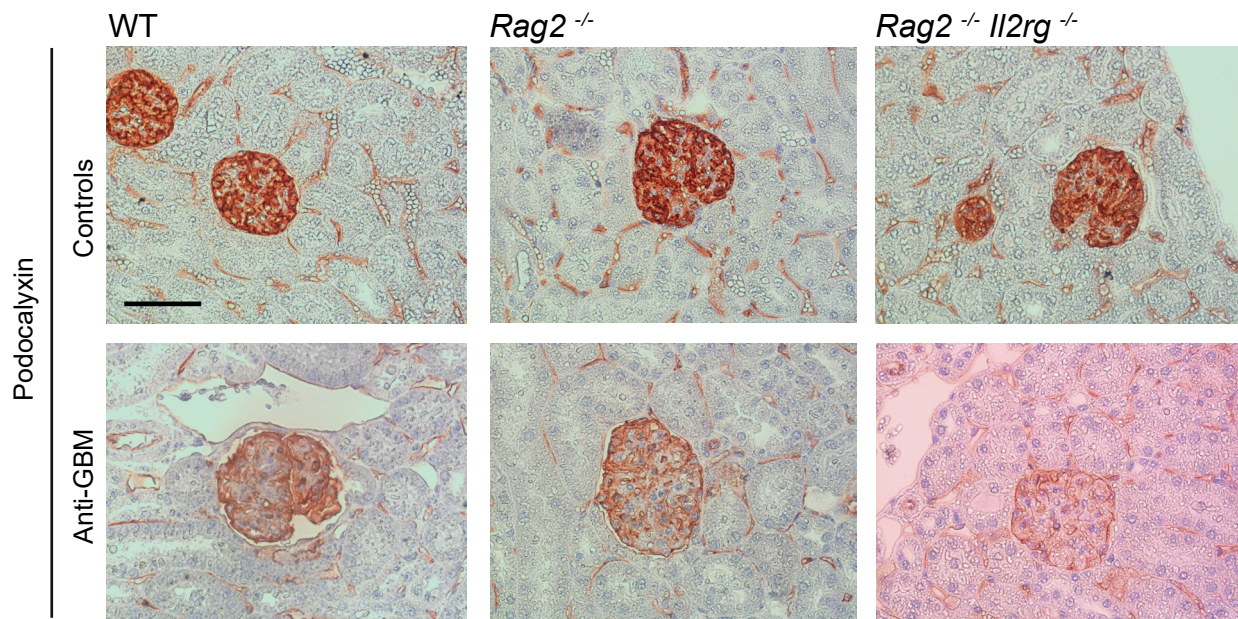
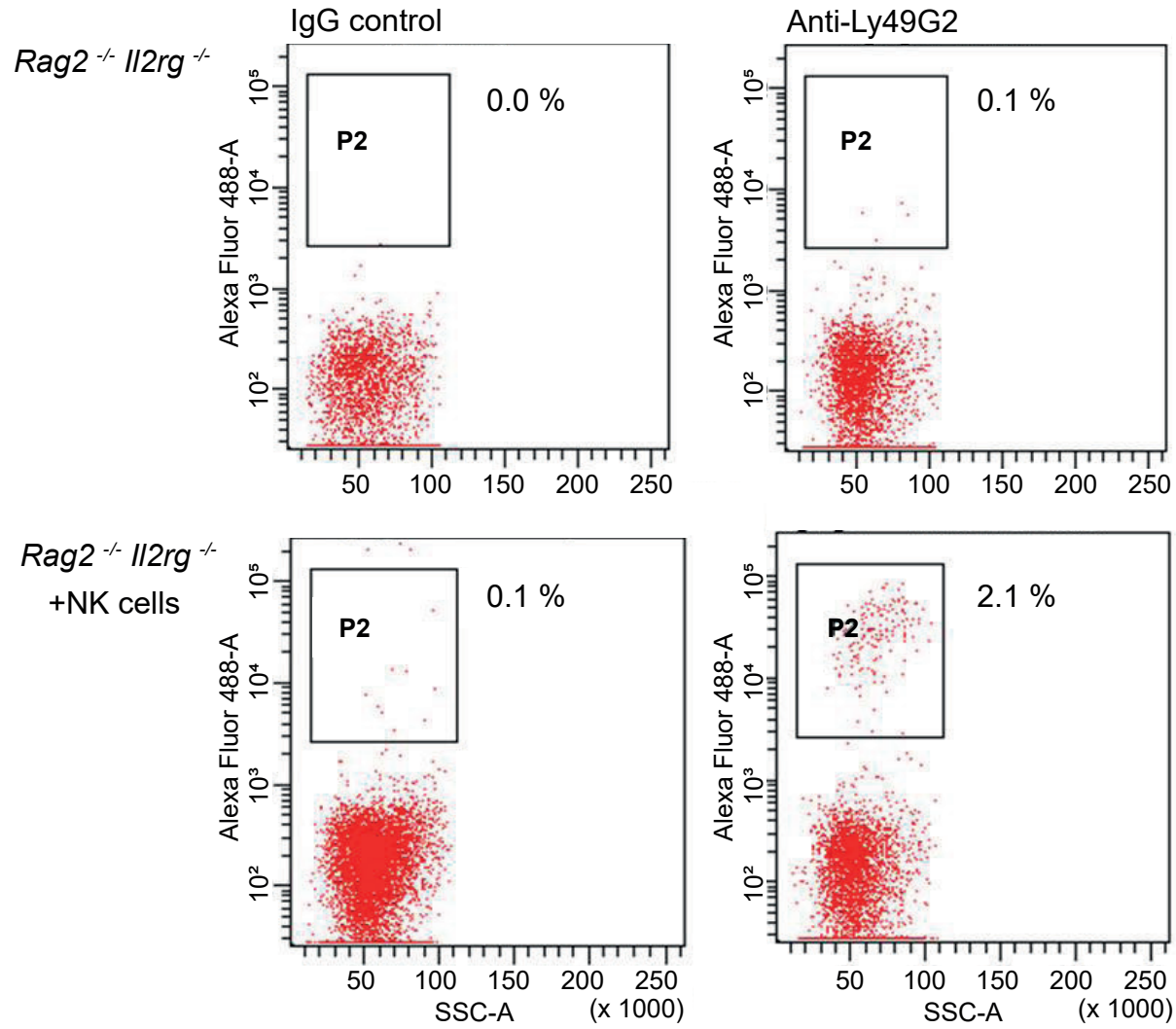
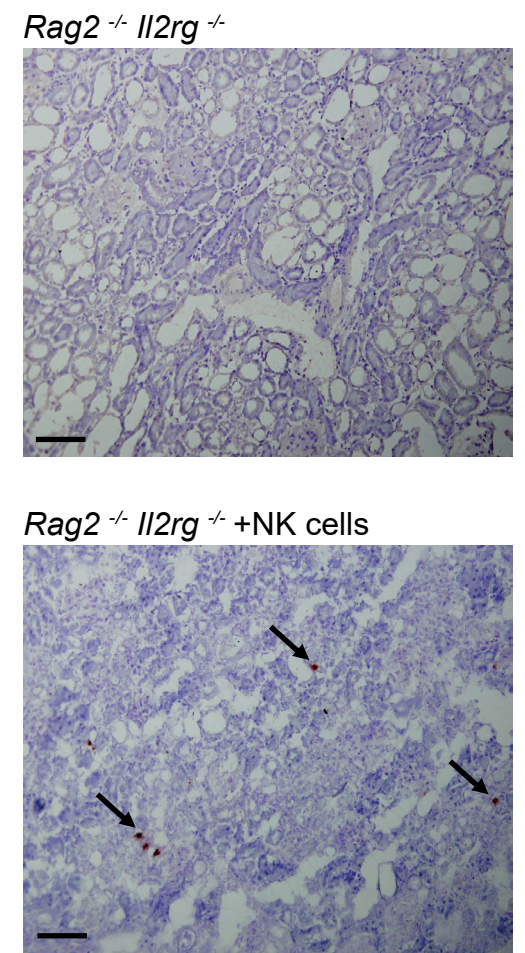


Figure 2 : Luque et al.

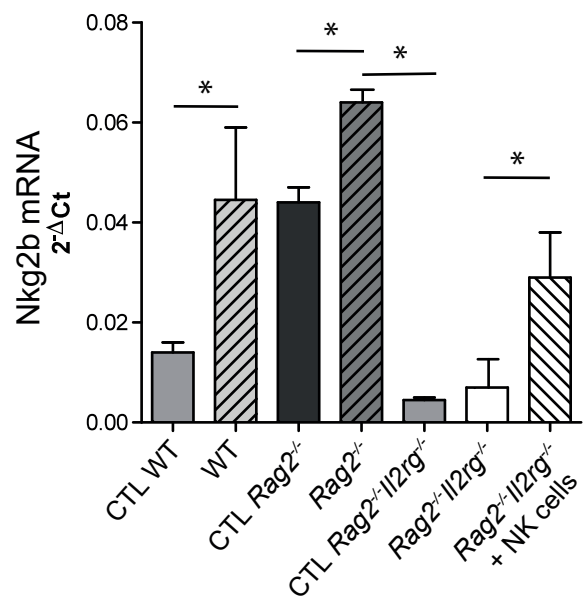
A



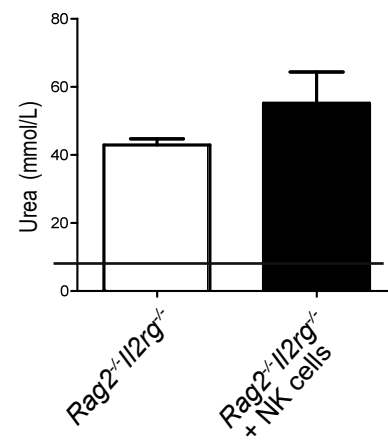
B



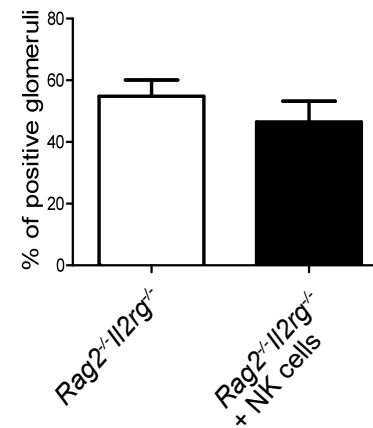
C



D



E



F

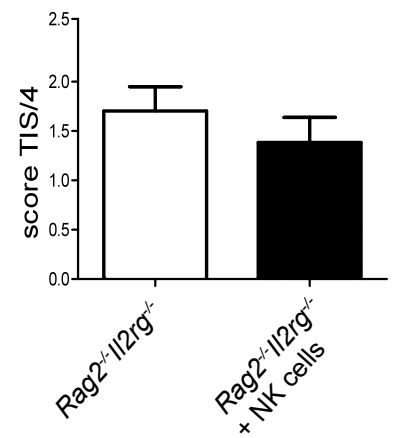


Figure 3: Luque et al.

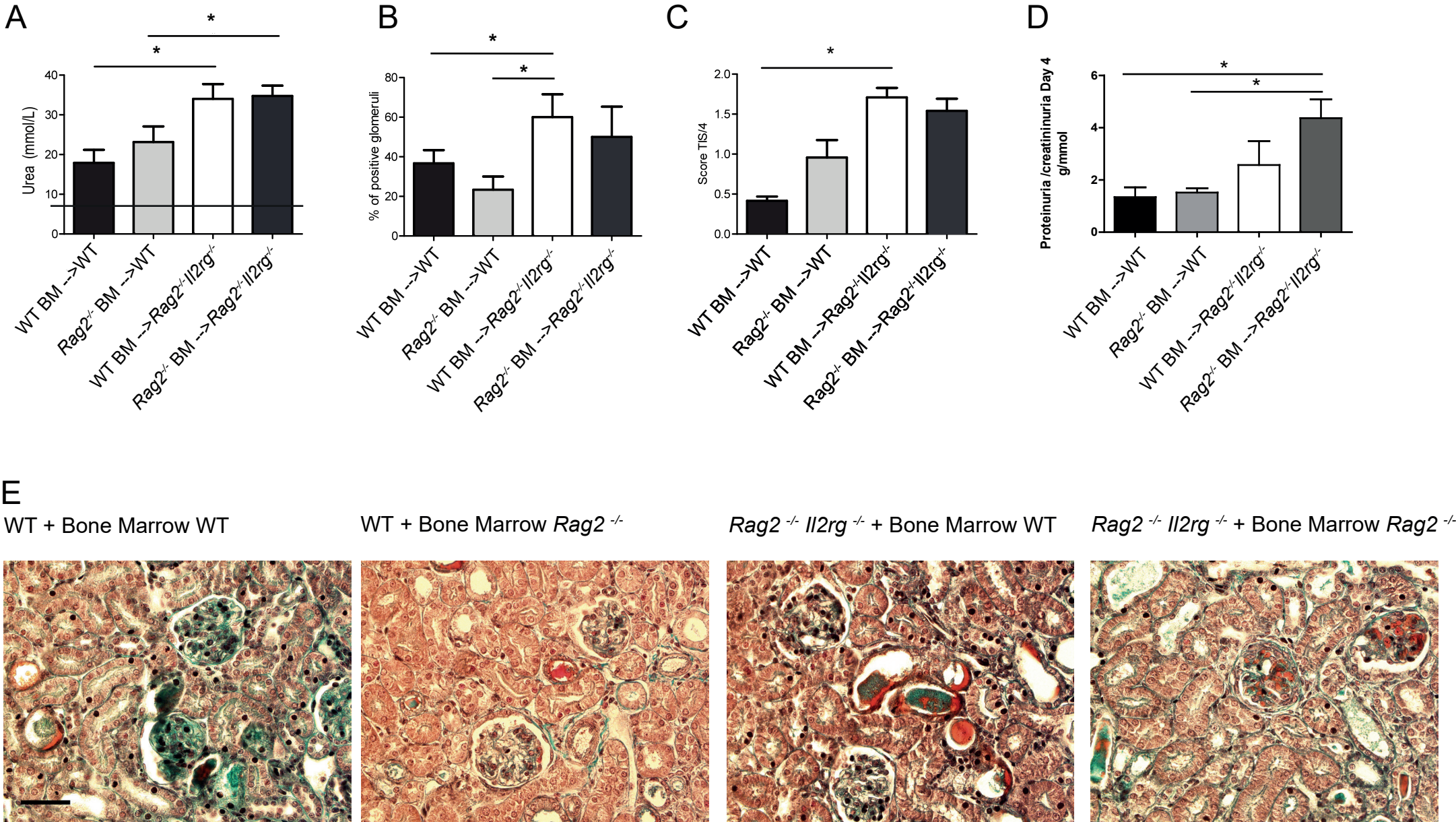
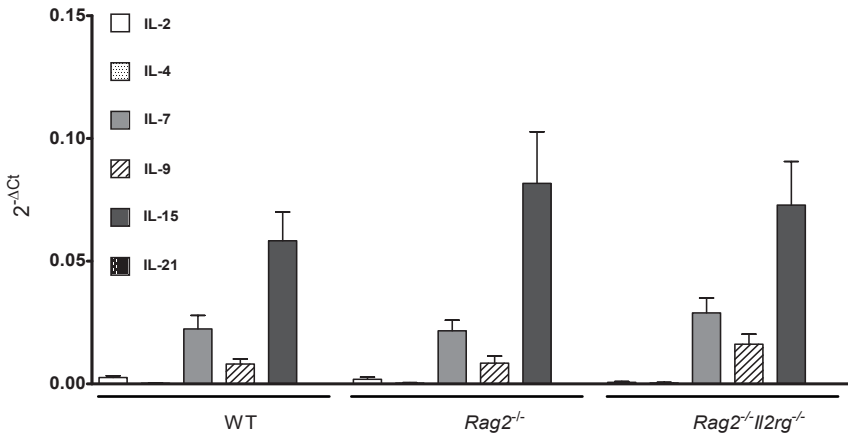
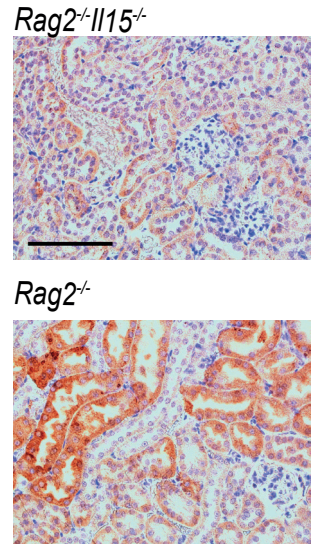


Figure 4: Luque et al.

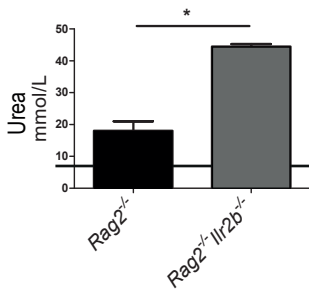
A



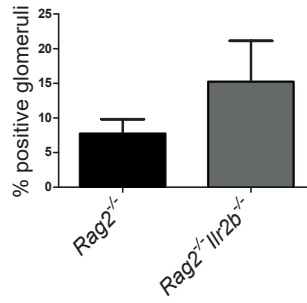
B



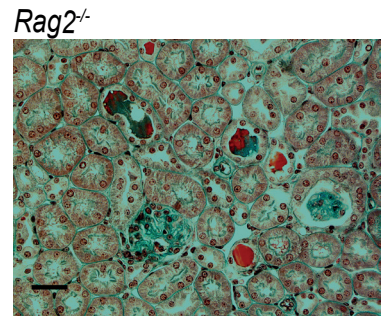
C



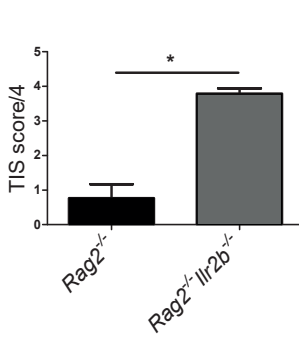
D



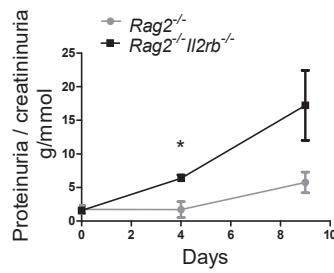
G



E



F



$Rag2^{-/-}Il1r2b^{-/-}$

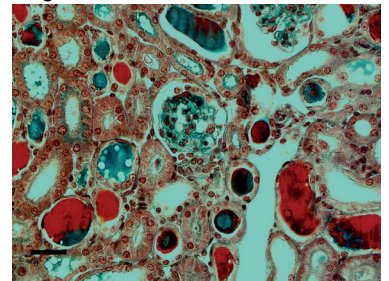
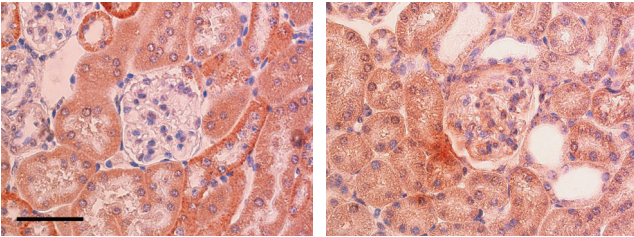


Figure 5: Luque et al.

A

IL-15R α CTL

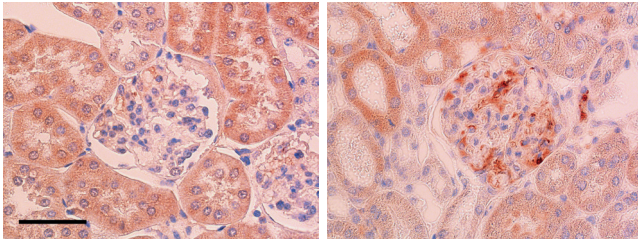
IL-15R α anti-GBM



B

IL-2R β CTL

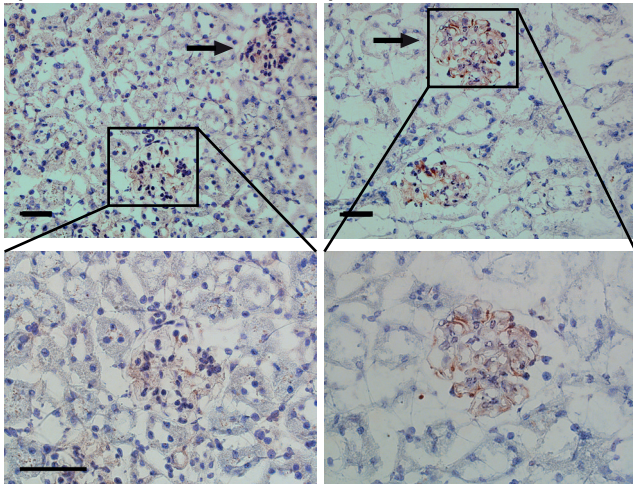
IL-2R β anti-GBM



C

γ C Chain CTL

γ C Chain anti-GBM



D

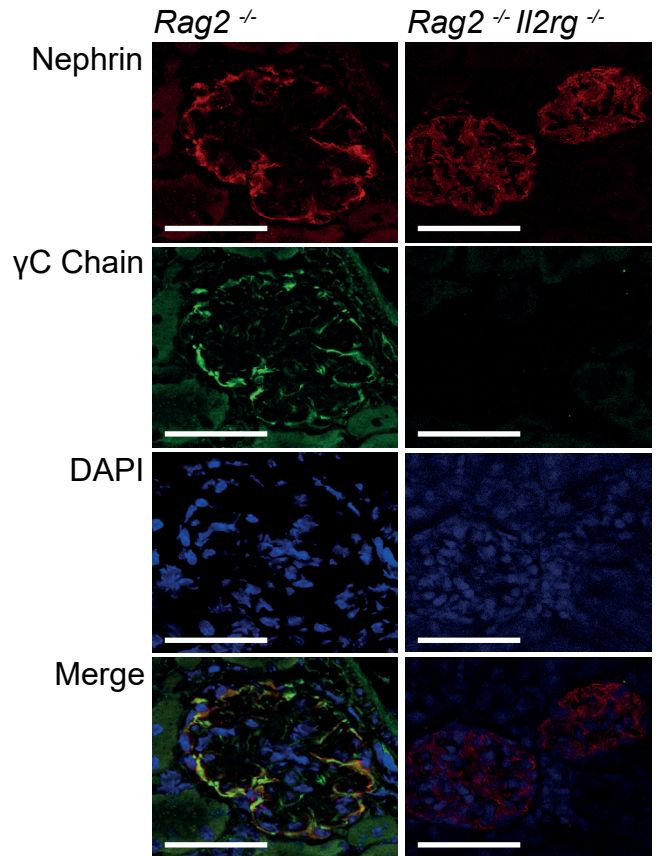


Figure 6: Luque et al.

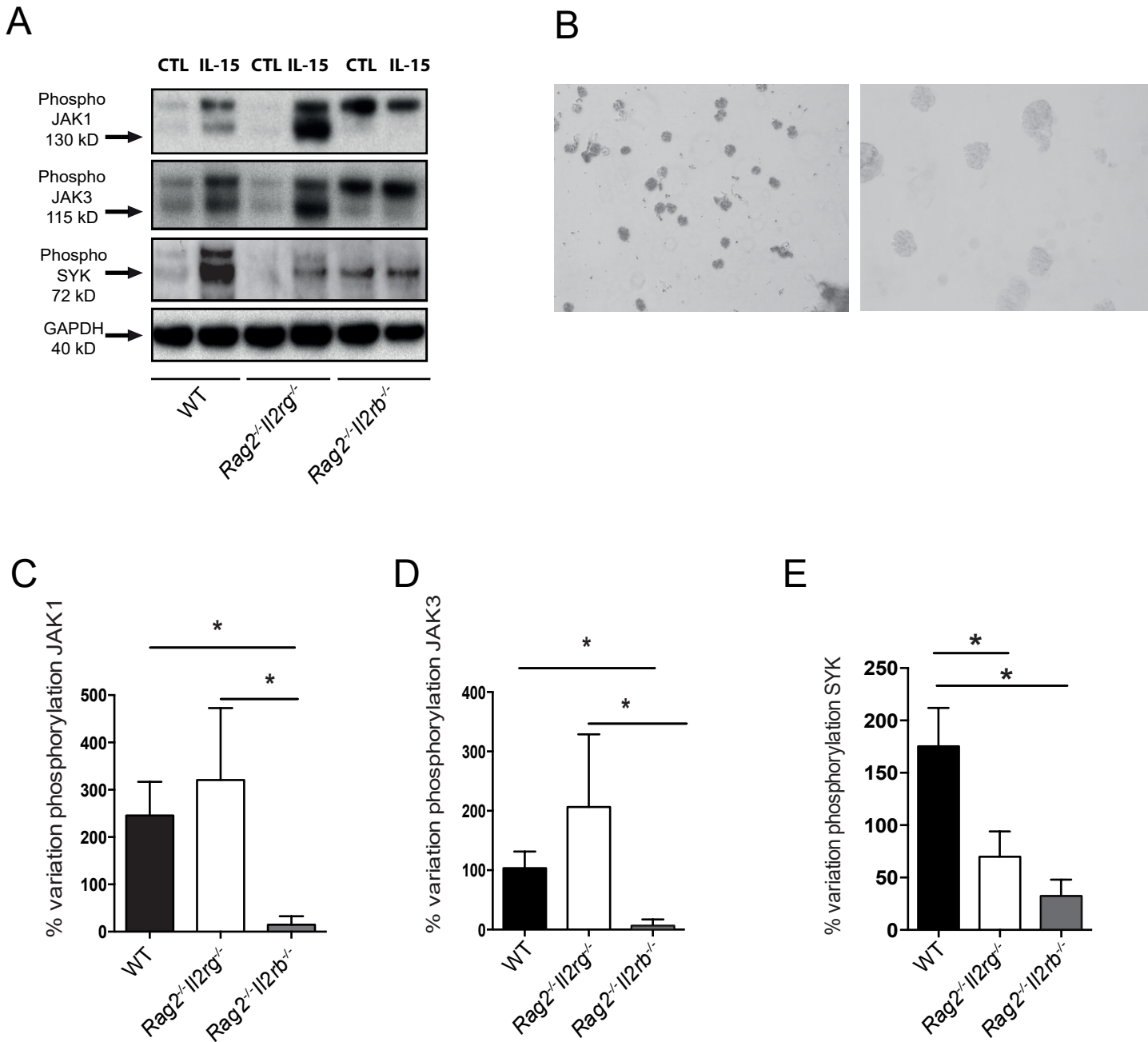
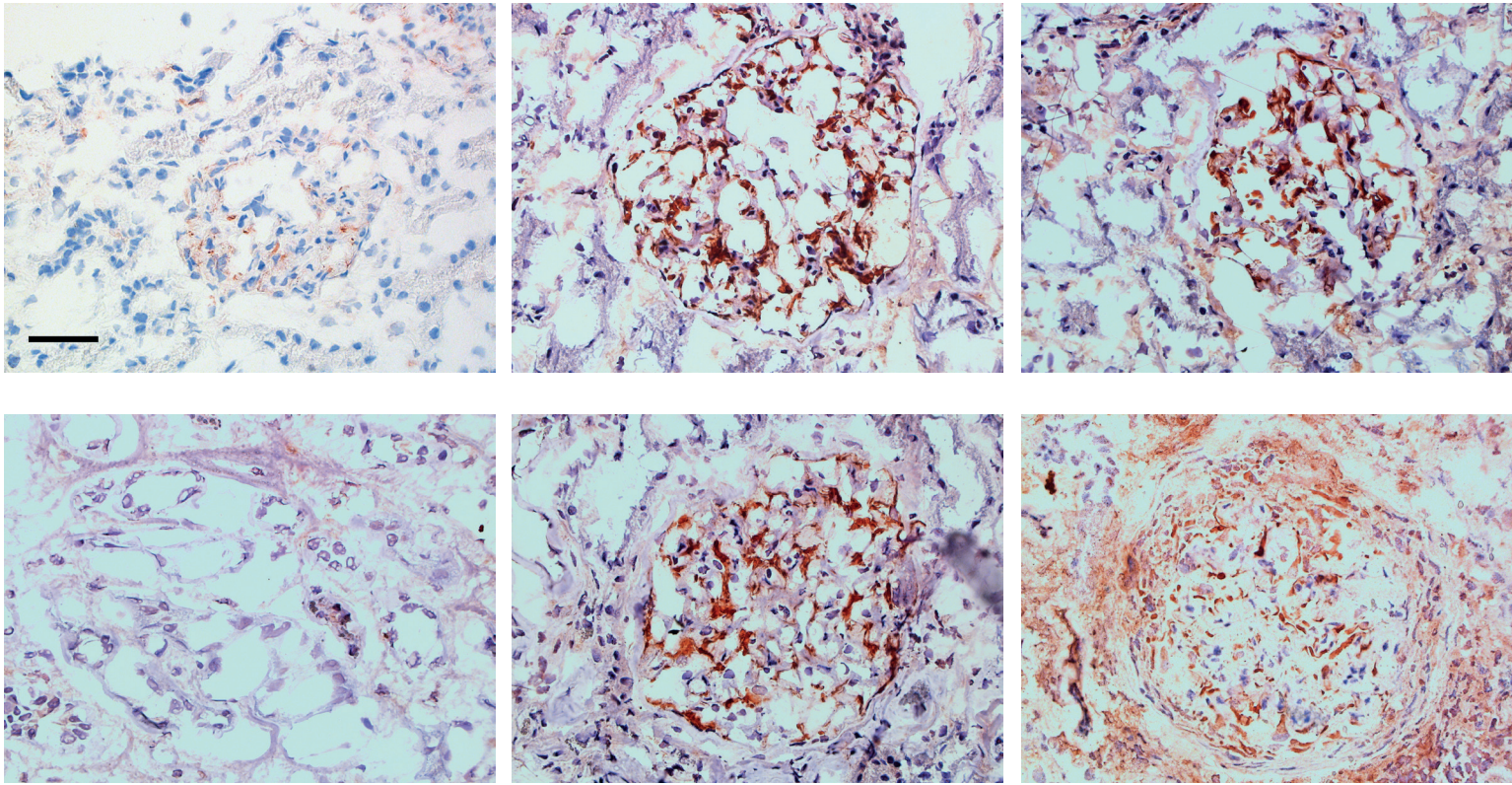


Figure 7: Luque et al.

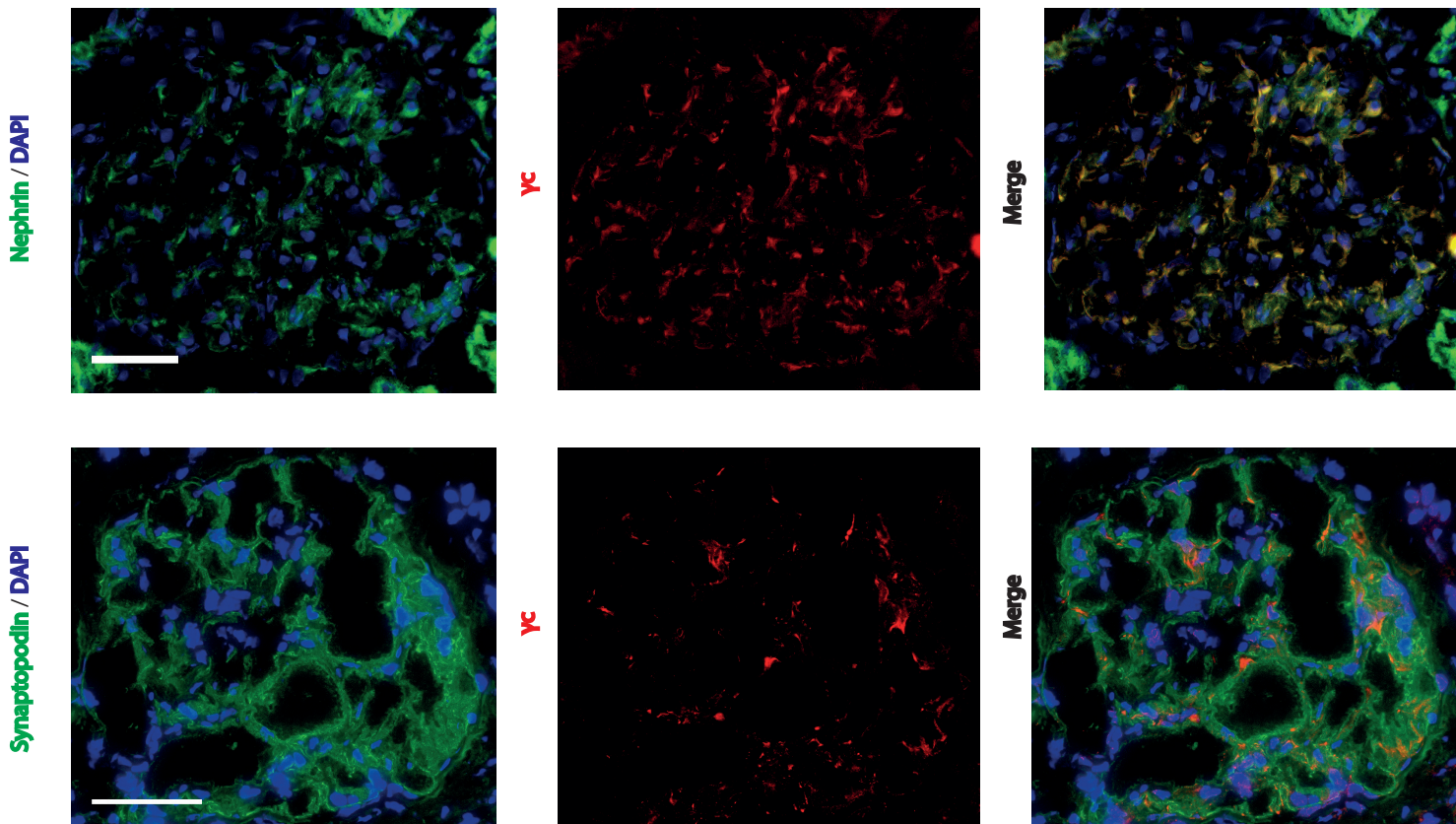
A

Pristine 3-month post-transplant renal biopsies

Human crescentic glomerulonephritis



B



Supplemental Table 1: Luque et al.

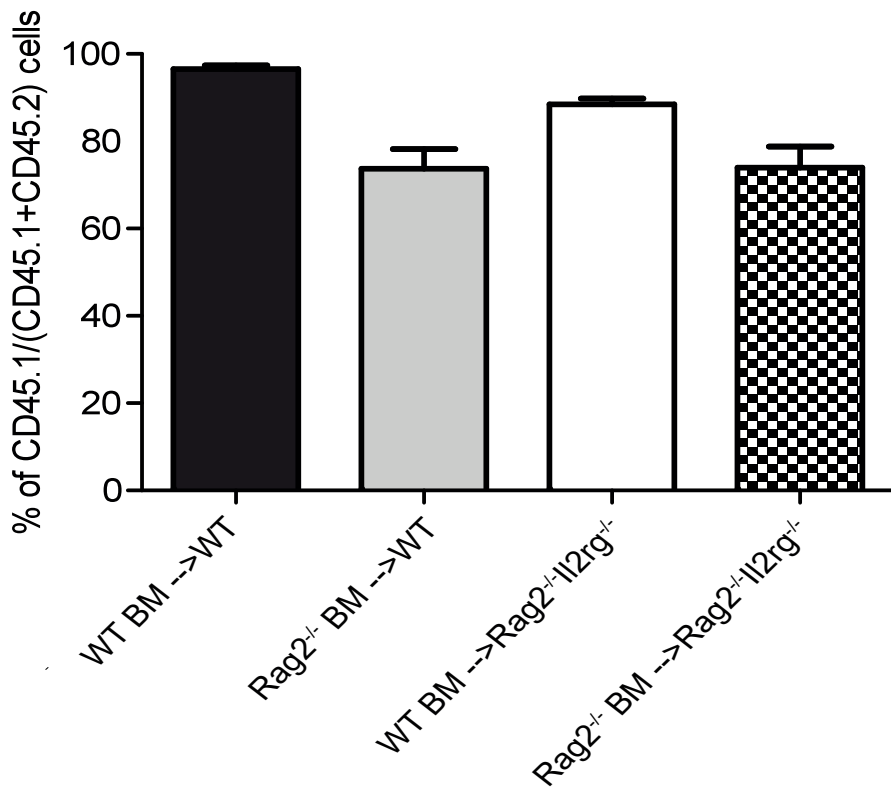
Transcript Name	Primer pairs
IL-2	5'-GCTGTTGATGGACCTACAGGA-3'
	5'-TTCAATTCTGTGGCCTGCTT-3'
IL-4	5'-CCTGCTCTTCTTTCTCGAATGT-3'
	5'-CACATCCATCTCCGTGCAT-3'
IL-7	5'-CGCAGACCATGTTCCATGT-3'
	5'-TCTTTAATGTGGCACTCAGATGAT-3'
IL-9	5'-GCCTCTGTTTTGCTCTTCAGTT-3'
	5'-GCATTTTGACGGTGGATCA-3'
IL-15	5'-CAGCTCAGAGAGGTCAGGAAA-3'
	5'-CATGAAGAGGCAGTGCTTTG-3'
IL-21	5'-GACATTCATCATTGACCTCGTG-3'
	5'-TCACAGGAAGGGCATTTAGC-3'
nkg2d	5'-CTCCTGGCAGTGGGAAGAT-3'
	5'-AAGCTTGAGCCATAGACAGCA- 3'
Gusb	5'-CTCTGGTGGCCTTACCTGAT-3
	5'-CAGTTGTTGTCACCTTCACCTC-3'

Mice	WT	<i>Rag2</i> ^{-/-}	<i>Rag2</i> ^{-/-} <i>Il2rg</i> ^{-/-}	<i>Rag2</i> ^{-/-} <i>Il2rb</i> ^{-/-}	<i>Rag2</i> ^{-/-} <i>Il15</i> ^{-/-}
Genetic background (N>12)	C57BL/6J	C57BL/6J	C57BL/6J	C57BL/6J	C57BL/6J
Body weight (g)**	23.1 ± 3.5	24.1 ± 4.1	23.1 ± 3.6	20.6 ± 1.1	19 ± 1.1
Kidney to body weight ratio	0.6 ± 0.1	0.6 ± 0.0	0.6 ± 0.0	0.6 ± 0.0	0.6 ± 0.0
Urea (mmol/L)	8.3 ± 2	10.9 ± 0.7	7.6 ± 0.7	8.8 ± 2.2	8.7 ± 0.3
Proteinuria to creatininuria ratio (g/mmol)*	1.1 ± 0.9	1.2 ± 1	0.7 ± 0.5	1.0 ± 0.7	0.5 ± 0.2

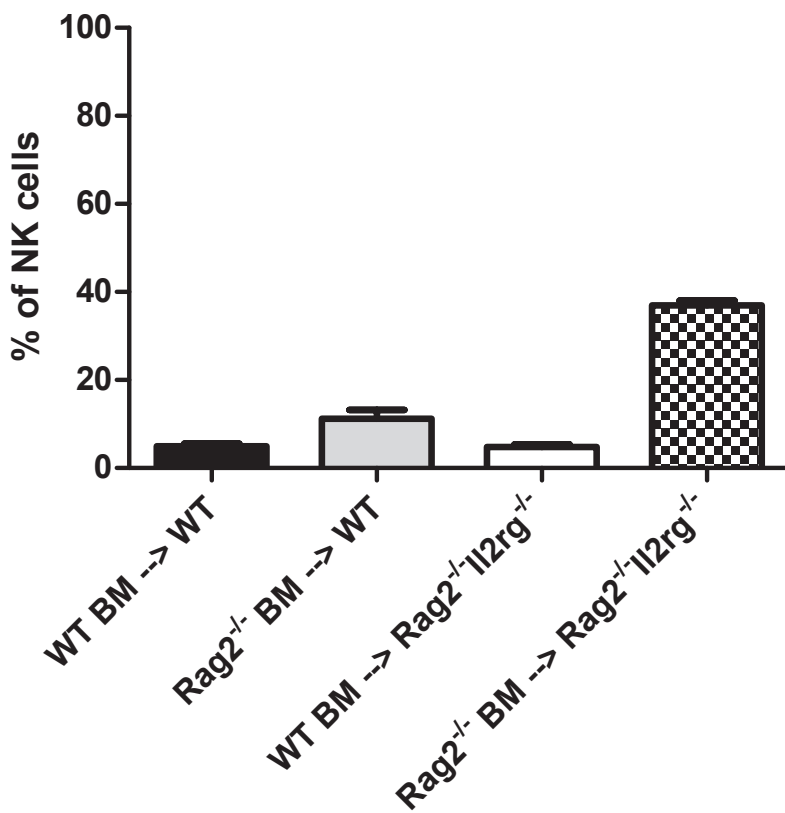
Supplemental Table 2: Phenotypic characteristics of different mice used in our study. Data represents means ± SEM of at least 5 mice per group. Kruskal-Wallis non-parametric test. * p<0.05, ** p<0.01.

Supplemental figure 1: Luque et al.

A

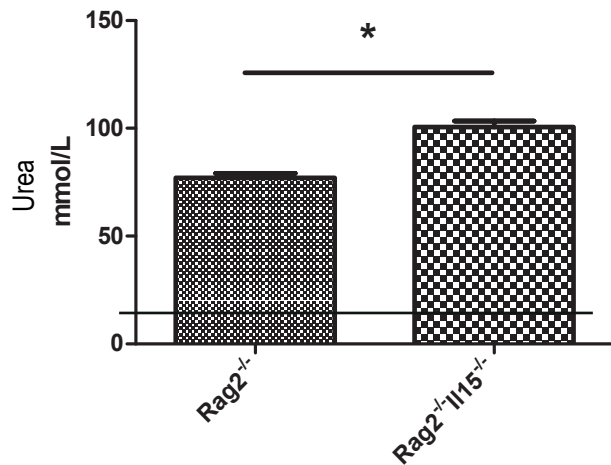


B



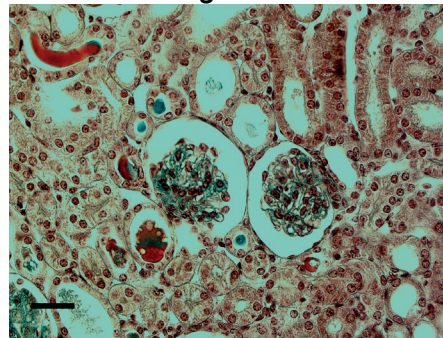
Supplemental figure 2: Luque et al.

A

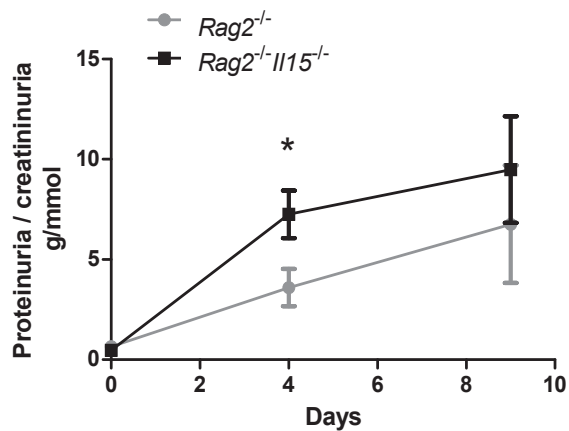


C

Anti-GBM- $Rag2^{-/-}$

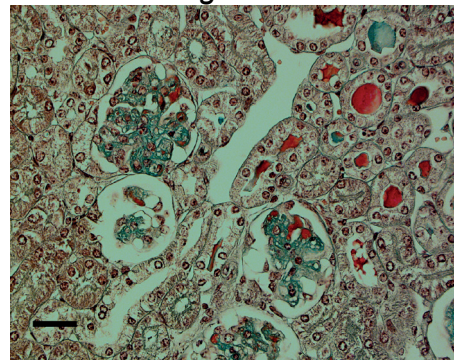


B



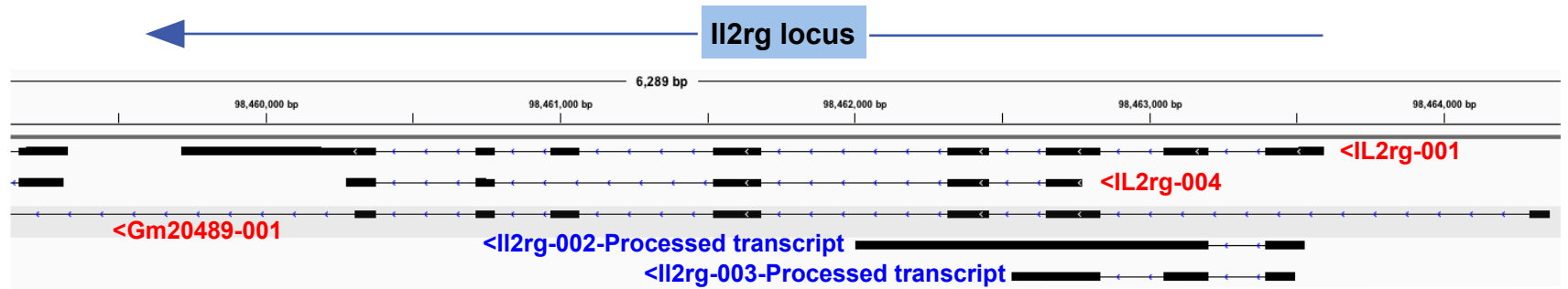
D

Anti-GBM- $Rag2^{-/-}Il15^{-/-}$

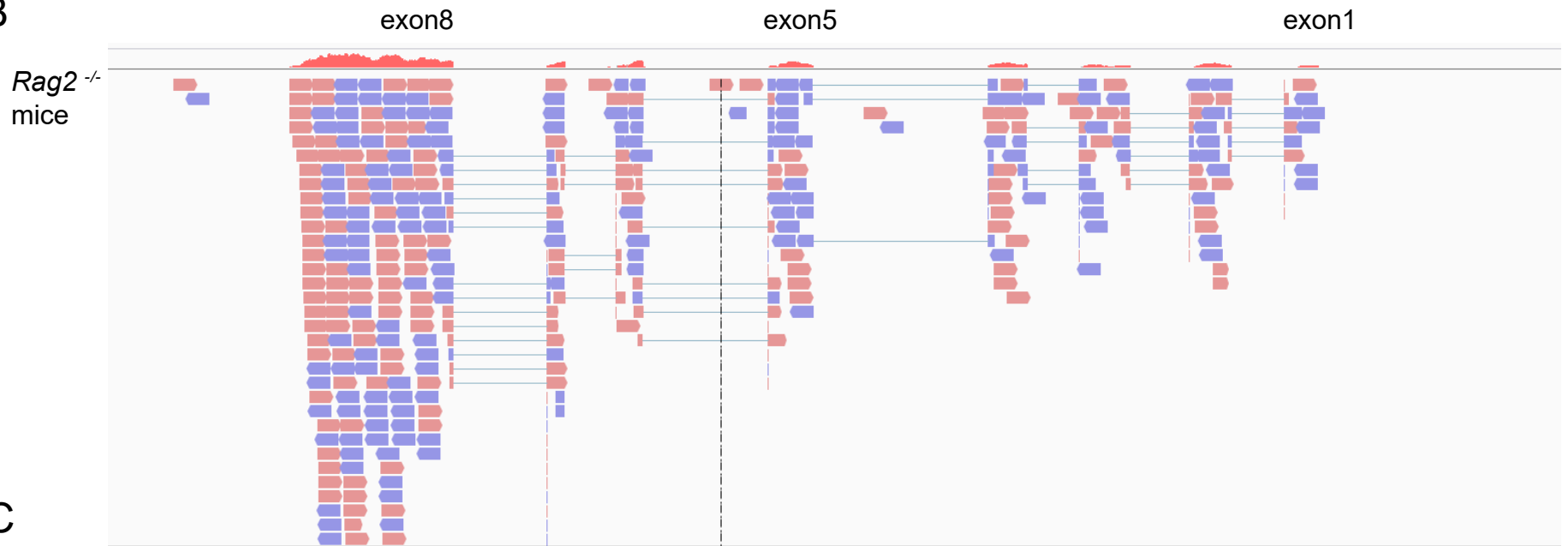


Supplemental figure 3: Luque et al.

A



B



C



Supplemental Figure 4: Luque et al.

